FLUORESCENCE CORRELATION SPECTROSCOPY: ULTRASENSITIVE DETECTION IN CLEAR AND TURBID MEDIA

BY

ABDEL KADER TAHARI

B.S., Université des Sciences et de la Technologie d'Alger, 1985
M.S., University of California, Riverside, 1987

DISSERTATION

Submitted in partial fulfillment of the requirements
for the degree of Doctor of Philosophy in Physics
in the graduate College of the
University of Illinois at Urbana-Champaign, 2006

Urbana, Illinois

FLUORESCENCE CORRELATION SPECTROSCOPY:
ULTRASENSITIVE DETECTION IN CLEAR AND TURBID MEDIA

Abdel K. Tahari, Ph.D.
Department of Physics
University of Illinois at Urbana-Champaign, 2005
Enrico Gratton, Advisor

In this work, I describe the development of a simple, inexpensive, and powerful alternative technique to detect and analyze, without enrichment, extremely low concentrations of cells, bacteria, viruses, and protein aggregates in turbid fluids for clinical and biotechnological applications. The anticipated applications of this technique are many. They range from the determination of the somatic cell count in milk for the dairy industry, to the enumeration and characterization of microorganisms in environmental microbiology and the food industry, and to the fast and ultrasensitive detection of protein aggregates for the diagnosis of Alzheimer's and other neurodegenerative diseases in clinical medicine. A prototype instrument has been built and allowed the detection and quantification of particles down to a few per milliliter in short scanning times. It consists of a small microscope that has a horizontal geometry and a mechanical instrument that holds a cylindrical cuvette (1 cm in diameter) with two motors that provide a rotational and a slower vertical inversion motions. The illumination focus is centered about 200 μm from the wall of the cuvette inside the sample. The total volume that is explored is large (~ 1ml/min for bright particles). The data is analyzed with a correlation filter program based on particle passage pattern recognition. I will also describe further work on improving the sensitivity of the technique, expanding it for multiple-species discrimination and enumeration, and testing the prototype device in actual clinical and biotechnological applications. The main clinical application of this project seeks to establish conditions and use this new technique to quantify and size-analyze oligomeric complexes of the Alzheimer's disease β-peptide in cerebrospinal fluid and other body fluids as a molecular biomarker for persons at risk of Alzheimer's disease dementia. The technology could potentially be extended to the diagnosis and therapeutic monitoring of other protein neurologic diseases where oligomeric forms may play a role.

To my mother and the memory of my father

Acknowledgments

I would like to acknowledge the assistance and thank the people who contributed directly or indirectly to make this work possible. The members of the Laboratory of Florescence Dynamics over the years have been of great help but are too numerous to mention by name. I would like to specifically thank Nick Barry, Bill Mantulin, Chip Hazlett, Julie Wright, Bob Clegg, and my advisor, Enrico Gratton.

This work was supported financially by the National Institutes of Health, Grants PHS 5 P41-RRO3155 and PHS 1 F30 NS48776-01A1, and by UIUC.

Table of Contents

Chapter 1 Introduction

Outline

This introductory chapter deals with the initial motivation for embarking on this research project. It begins by stressing the importance of fast detection of cells, bacteria, and diverse other particles in medicine, biotechnology, and many other fields. It briefly describes some of the conventional techniques and their shortcomings. A special attention is given to flow cytometry, its advantages and drawbacks. The need for a new instrument and detection technique is highlighted. This is followed by an outline of the organization of the rest of the dissertation.

Significance of Fast Detection

The importance of fast and efficient screening for single particles has increased significantly for applications in biotechnology and medicine in recent times. The particles may be single eukaryotic cells with particular properties, bacteria, viruses, protein aggregates, or even molecular entities such as peptide hormones or other oligomeric compounds (Meyer and Schindler 1988; Rigler 1995). In some instances there is a need for the detection of extremely low concentrations of particular entities such as in the diagnosis of a disease in its early stages by the direct detection of viruses in body fluids in the initial phase of infection, especially when there is a long gap between infection and the response of the immune system, or the fast screening for virulent forms of bacteria or other pathogens in food stuffs and drinking water.

As an example, each year, foodborne contamination with E. coli O157:H7 alone results in approximately 62,500 illnesses, requires 1,843 hospitalizations, and causes 52 deaths (Tortora, Funke et al. 1998). Many methods exist for the detection of E. coli O157:H7 in food and water. These detection systems include cultural techniques, immunological procedures, and nucleic acid-based assays. However, most of these tests require a combination of long incubation times to grow the bacteria to high enough levels for detection, meaning that test results are not known for several days. In the time interval required to obtain a test result, contaminated food may have already been disseminated to retail stores and purchased by consumers. In addition, these tests are expensive and often quite complex, requiring intensive training for laboratory personnel. Therefore, there remains a need for very sensitive, rapid, and simple methods capable of detecting food pathogens.

Conventional Detection Techniques and Their Shortcomings

Traditionally, the detection and estimation of low concentrations of microorganisms has relied on diverse culturing techniques. The procedures are often lengthy and not easily amenable to the detection of trace amounts. Conventional testing methods for microorganisms are also relatively costly and time-consuming. The most common testing method requires taking a product sample, then culturing that sample until enough microorganisms exist to be readily detected on differential culture plates or using conventional immunoassays, a process that can take several days. Other methods may provide faster detection but require complicated procedures, expensive reagents and equipment, and extensively trained personnel. Nearly all of these methods require

samples to be manually collected on the plant floor and taken to a laboratory for subsequent analysis.

Some methods yield a *total cell count* taking no account of whether the microbes are viable or not. These include (Heritage, Evans et al. 1996):

Turbidimetric method: This method uses the ability of the microorganisms to scatter light. Spectrophotometers measure the dispersal of light by placing the sample in line between a light source and a detector and comparing it to an appropriate blank. Because bacteria vary in light scattering properties, standard curves, using alternative counting methods, must be prepared of turbidity against cell numbers. This method obviously works only for very large concentrations of microorganisms.

Wet and Dry weight method: Suspensions of microbes may be harvested by centrifugation, and the weight of the cells determined. However, the quantity of liquid trapped can vary, influencing the outcome. The *dry weight*, measured after repeated desiccation steps, could be measured for a better estimate. By itself, this method is also not suited for the detection of trace amounts of bacteria.

Microscopic counting methods: Bacteria may be counted directly by observing them in a microscope. This is typically done by placing a suspension in a counting chamber. These are specially made glass slides with an accurately etched grid in the middle of the slide. When a cover slip is placed on the slide, a known volume of the suspension is trapped. The mean number in each square grid is determined by direct counting and the concentration of the organisms in the original sample is then deduced. The motility of the microbes complicates the process as it makes counting in the different grids difficult and sometimes impossible.

Alternatively, other methods try to estimate the *viable cell count* to determine the number of organisms capable of propagating themselves. These methods include (Heritage, Evans et al. 1996):

Chemical analysis methods: The growing bacteria produce macromolecules from subunits present in the growth medium. One method uses the enzyme *luciferase* which produces light from the hydrolysis of ATP. The number of bacteria present in the sample may be estimated by measuring the bioluminescence of the suspension.

Spread plate techniques: The initial inoculum is subjected to a serial dilution until very few bacteria are expected in the dilutent. A small sample with known volume is removed from many dilution tubes and each placed on the surface of an appropriate growth medium in a Petri dish. Sterile spreaders and stringent septic techniques are required to avoid contamination with other unwanted microorganisms. The cultures are incubated and colonies are allowed to form. The technique is error prone and takes a considerable time to perform, notwithstanding the fact that it is considered the *gold standard* of counting of bacteria.

The *pour-plate method*, the *spiral platter*, and the *method of Miles and Misra*, are variations of the plate counting method sometimes used when a relatively more precise or more economic evaluation of the bacteria concentration is sought (Heritage, Evans et al. 1996).

In addition to being very tedious and requiring stringent sterile methodologies, the failure of bacteria to form colonies is a problem when using plate counting procedures (McFeters, Yu et al. 1995). This concern was recognized early by Winogradsky

(Winogradsky 1949), and more recently by others (Atlas 1984; Ward, Bateson et al. 1992; McDougald, Rice et al. 1998). Additional problems with plate counts include:

- lengthy incubation times are required for colonies to become visible
- cell clumping can lead to an undercount of viable cells
- it is very easy to have too many or too few colonies on a plate to accurately measure viable count
- too low a concentration requires enrichment steps

As a result, the ability to describe microbial populations using methods based on colony formation is both flawed and time-consuming.

Measurements of bacteria and other microorganisms at the level of single cells have progressed enormously in the last few decades. Up to the late 1970's, there were no other means than microscopy for the observation of single microorganisms, making any type of measurement very cumbersome and tedious. For the detection of low concentrations, traditional microscopy is totally inadequate, as the probability of observing a microbe in a random specimen is extremely small.

A spectrum of alternative methodologies is now available to detect and quantify microorganisms. These include immunological methods, image analysis technology, cellular biochemical signatures, microcalorimetry and microelectrodes (Tunlid and White 1992; Paul 1993). However, most of these technologies carry with them disadvantages that are recognized in the design and interpretations of experiments where they are used. Most of these techniques provide estimated averages over the entire samples so that

differences between cells and heterogeneities cannot be resolved (McFeters, Yu et al. 1995).

Some of the most familiar techniques that were developed since the 1970's include (Jay 1992):

Polymerase Chain Reaction (PCR): This technique is more applicable to the detection of organisms than to their enumeration. By employing thermostable DNA polymerases and 5' and 3' specific oligonucleotide primers, a single molecule of DNA can be amplified to 10^7 molecules after a series of amplification cycles, usually 40 to 50 cycles. Agarose gels or Southern hybridization techniques are then employed to detect this amplified DNA. PCR requires a very clean work environment since contaminating DNA can be amplified, along with that from the organism of interest.

Radioimmunoassay (RIA): This technique consists of adding a radioactive label to an antigen, allowing the antigen to react with its specific antibody, then measuring the amount of antigen that combined with the antibody by use of a counter to measure total radioactivity. Usually solid-phase RIA is employed in which a monolayer of antibody molecules is bound electrostatically to a solid material. Free labeled antigen is washed out before radioactivity is measured.

Enzyme-Linked Immunosorbent Assay (ELISA): It is an immunological method similar to RIA that uses an enzyme coupled to either antigen or antibody rather than a radioactive isotope. Typically a solid phase (polystyrene) is coated with antigen and incubated with antiserum. Following washing, an enzyme-labeled preparation of anti-immunoglobulin is added. After another cycle of washing, the enzyme remaining is assayed to determine the amount of antibodies in the initial serum. A commonly used

enzyme is horseradish peroxidase, and its presence is measured by the addition of peroxidase substrate. The amount of the latter is determined usually colorimetrically. Many variations of ELISA exist. The sensitivity threshold of these methods is usually around 10^7 cells/ml (Jay 1992).

Table 1.1 gives a summary of various existing detection techniques and their limitations.

Technique	**Example**	**Limitations**
Selective media and culturing (traditional)	Spread plate, spiral platter	Long processing time, labor intensive, finite selective media
Microscopical	Direct epifluorescent filter technique (DEFT)	Labor intensive, selective media, detection limit 10^3/ml, limited organism range
Nucleic acid based assays	Labeled DNA probes PCR	Enrichment, cross-species reactivity leading to false positives, lengthy manipulation
Antibody based assays	ELISA, immunoprecipitation, agglutination	Low sensitivity (10^{5-7}/ml), enrichment needed, considerable manipulation, debris interference
Electric methods	Impedance- based detection	Variability, altered growth rates, temperature sensitive
Physically-based	Immunodiffusion	Restricted to motile organisms, variability
Biochemical assays	ATP, β-gal activity, gas chromatography	Non-selective, low sensitivity, somatic ATP interference, non-specificity to pathogens, pure cultures needed
Flow Cytometry		limited size range, may require enrichment, difficult calibration, clogging from debris, trained labor required, high cost

Table 1.1 Summary of various existing detection techniques and their limitations

Flow Cytometry: Concepts and Disadvantages

Cell cytometry began with the development of the Coulter Counter in the 1950's (Coulter 1956). The Coulter Counter detects changes in electrical conductivity of a small saline orifice as cells pass through it. It provides a good estimate of cell volume, but the method lacks sensitivity for small bacteria and is subject to interference from debris (Porter, Pickup et al. 1997). Flow Cytometry was developed in the late 1960's. It consists of the measurement of cellular properties as they are moving in a fluid stream past a stationary set of detectors (Shapiro 1995). Typically, the cell sample is introduced into the center of a stream of sheath fluid. The sheath fluid is pumped much faster than the sample in a process known as hydrodynamic focusing. Measurements of the cells, flowing in a single file fashion, are made by exciting them, most commonly with a laser, and an optical sensor measures the light scattered by the cell or particle. Labeled probes and a plethora of fluorescent dyes aid in the detection of a variety of cell types and cell components. Optical flow cytometry techniques allow individual cells to be distinguished on the basis of a large number of parameters, such as their size, quantity of granular structures, and the presence and abundance of detectable markers. As a result of this capability, optical flow cytometers are often used to generate a diagnostic profile of a population of particles in a biological sample. For example, flow cytometry has been effectively used to measure the decline or maintenance of immune cells during the course of treatment for HIV infection and to determine the presence or absence of tumor cells for prognosis and diagnosis of cancer patients.

For a long time however, commercial flow cytometers were designed to study eukaryotic, mainly mammalian, cells (> 10 μm in diameter). High background noise from

large observation volumes results in the difficulty of detecting signals from the much smaller bacteria. In the last decade or so, continually improving technologies has resulted in flow cytometry laser-based instruments that are successfully applied to the study of microorganisms (Shapiro 1995; Davy and Kell 1996).

While Flow Cytometry is a powerful and versatile technique that can be applied to many biological questions, there are many limitations and drawbacks to the technology. First, the dynamic range, in term of the size of the entities to be studied, is narrow. As a consequence, different machines are designed for studying different cell size ranges. Second, the user must ensure that there are no clumps of cells or other debris present in the sample as these could block the flow cell. Therefore, samples and sheath fluids need to be carefully filtered to prevent obstruction of the flow, which is often troublesome and hard to correct. Third, because of their complexity, skilled operators are required to use them. Alignment and calibration of the flow cytometers are not simple tasks, and need to be performed frequently. Fourth, it is necessary for the unit to be routinely cleaned and the tubing flushed and disinfected to prevent bio-film buildup and contamination, especially when working with microorganisms. Fifth, the sample studied is lost in most flow systems, and therefore cannot be used for additional analysis using other techniques. This is a significant disadvantage especially for hard-to-get and expensive samples (Shapiro 1995; Schwartz, Marti. et al. 1998; Edwards 1999). The substantial cost of the machines, even the ones not capable of cell sorting, in addition to their non-portability, is a big disadvantage and has prevented the widespread use of this technology outside research and clinical institutions.

Need for a New Instrument and Data Analysis Technique

It is clear from the foregoing discussion that there is currently a need for optical methods and devices for identifying and characterizing components of sample present in extremely low quantities, particularly trace components of biological samples. Optical analysis methods and devices providing a large dynamic range with respect to the size distribution, composition and physical state of particles analyzed are needed. In addition, optical analysis methods and devices are needed that are less susceptible to bio-film buildup and contamination than conventional optical flow cytometers, and which do not require cumbersome pre-filtration of samples undergoing analysis. Finally, inexpensive, simple, and portable optical analysis devices are needed for analyzing biological samples, which can be operated by individuals without extensive training.

In this dissertation, I will describe an alternative system for the detection and enumeration of extremely low concentrations of fluorescently-tagged particles in both clear and scattering media. The technical methods and the device built aim for large dynamic range in terms of the size of the entities to be studied, low cost, simplicity, and portability. In addition to describing the instrument and the techniques used for detecting particles in a sample and measuring concentrations, I will describe the application-driven evolution of the system to the present status where it can also determine the size distribution of the entities measured, and ideas about possible future expansions.

I have chosen to follow a chronological path in writing this dissertation. I believe this will provide a clearer and more logical explanation of the thought process, the reasoning behind trying diverse techniques, starting with FCS, spending some time with PCH, the outcomes and limitations of these before changing gear to look for a more

successful alternative in the applications sought. This effort led to the pattern recognition based filtration method of detection and enumeration. This, in addition to the simple and novel mechanical setup that provides for the scanning of the sample for handling the very low concentrations, a goal set from the outset. Finally, how the collaboration on the detection of Amyloid β gave the incentive to expand the technique for size-distribution determination. This work is in a category quite different from the application oriented projects where one uses a commercial instrument and applies a mature technique to a biological problem.

In the next chapter, I introduce the concept of fluorescence and give a basic and quick overview of the methods of FCS and PCH. The fact that both the autocorrelation function and the histogram depend on the concentration was the reason why these methods were first considered.

In chapter 3 I discuss a real life application and candidate for our instrument. The importance of the determination of the somatic cell count (SCC) in milk is briefly explained. This is followed by a discussion of the mechanical and optical components of our experimental setup. Calibration with fluorospheres both in clear and turbid media using a variant of PCH is explained. Results with SCC in milk will be presented. A discussion of the advantages and limitations of the method follows.

In chapter 4 I introduce the novel data filtration program that enabled us to reach detection in the attomolar range in reasonably short times. I describe how the algorithms work and discuss their advantages and the many obstacles they helped us conquer.

In chapter 5 I present experimental results obtained with the setup and the correlation filter. I describe a biotechnological application very important to the food

industry which deals with the detection of trace amounts of virulent bacteria in food matrices using fluorescently-tagged antibodies. This is followed by a discussion of the usefulness of the setup and the detection technique.

In chapter 6 I describe an ongoing collaboration that required us to further develop and advance the setup and the detection program. I introduce the clinical objective of finding a diagnostic marker for the progression of Alzheimer's disease. A potential candidate is the size distribution of soluble oligomers of β-Amyloid protein in cerebrospinal fluid and, ultimately, in blood plasma. I describe the modifications introduced in the setup and the new size characterization capability of the filter. Some preliminary results are presented.

In the last chapter I briefly discuss examples of many potential applications of the device and methods. I describe some possible and useful expansions such as multichannel setup and multi-slit confocal aperture.

Chapter 2 From Molecular FCS to Large Volume Scanning

Outline

This chapter begins by introducing the concept and usefulness of fluorescence. A quick overview of the fluctuation-based methods of FCS (Fluorescence Correlation Spectroscopy) and PCH (Photon Counting Histograms) follows. The dependence of both the autocorrelation function at time zero and the histograms on the number density provided the initial motivation and reason why these were considered.

Introduction

Fluorescence is a highly specific and sensitive property that is frequently used to identify molecules. It is a biphasic reaction between light quanta and resonant molecules. A photon of wavelength λ_e is taken up by a molecule producing an excited state with a lifetime in the nanosecond range. In the second phase, another photon with wavelength $\lambda_f > \lambda_e$ is emitted. The difference $\lambda_f - \lambda_e$, called the *Stokes shift*, is what makes fluorescence practical and very useful. Depending on the magnitude of this shift, the excitation light can be more or less easily filtered out to make the fluorescence emission measurable. Mainly due to the fact that efficient fluorescent dyes are used as specific tags in a wide spectrum of reactions, this method has become a very powerful tool in biological and organic chemistry. Labeled probes and a plethora of fluorescent dyes, stains and intercalators aid in the detection of a wide variety of cell types and cell components. In some methods, fluorescent antibodies are used to measure the densities

of specific surface receptors of cellular analytes, and thus to distinguish subpopulations of differentiated cell types. Intracellular components are also routinely detected and quantified using fluorescent probes in combination with optical flow cytometry, including total intracellular DNA, specific nucleotide sequences in DNA or mRNA, selected peptides and proteins and free fatty acids (Tsien and Waggoner 1995; Shapiro 2000).

Nonetheless, difficulty arises when working with turbid media like milk, blood, and other clinical fluids, where there is a high degree of scattering in both excitation light and fluorescence emission. However, during experiments done at our laboratory with tissues that strongly scatter light, it was realized that fluctuation analysis could be done and information about systems extracted (Cerrusi 1999; Walker 1999).

The usual way to record fluorescence signals is to illuminate a sufficiently large volume and to carefully separate the emitted fluorescence from the scattered light and other undesired luminescence. In average intensity methods, the background noise sets a finite resolution limit. It is practically difficult to measure subnanomolar concentrations ($\sim 10^{12}$ particles/ml) with these methods (Eigen and Rigler 1994).

In order to eliminate this limitation, we must avoid averaging over space and time. It is the superposition of the noise and the desired signal from the particles inherent in averaging that masks the desired single particle events. We must record signals from space elements that are small enough to host single particles and record fluctuations in the signal with adequate temporal resolution. Focusing light into space elements of the order of femtoliter or smaller is possible with confocal optics coupled to laser light

sources. Also time resolved recording down to subnanosecond regimes are easily achieved by modern techniques.

In diffusion or scanning based techniques, most of the time the observation volume is free of fluorescent particles and only noise is recorded. Occasionally a particle moves into the illuminated volume and emits a burst of fluorescence photons. These bursts can be identified by autocorrelating the time-resolved signal. This is the basis of the Fluorescence Correlation Spectroscopy (FCS) technique.

The FCS Method

In the FCS method, one extracts information about the sample by analyzing the fluorescence signal fluctuations arising from a microscopic sub-volume. Random fluctuations of fluorescence intensity from single molecules provide information on important molecular properties such as translational and rotational diffusion, chemical kinetics, and the lifetime of the excited state (Elson and Magde 1974; Elson, Magde et al. 1974).

The signal $I(t)$ generated by molecules traversing the observation volume will fluctuate around a mean value $\langle I \rangle$. The autocorrelation function is

$$G(\tau) = \frac{\langle \delta I(t) \cdot \delta I(t+\tau) \rangle}{\langle I \rangle^2}$$

It can be shown (Thompson 1991) that $G(0)$ is inversely proportional to the number of particles in the excitation volume, and therefore to the concentration of particles in the sample,

$$G(0) = \frac{\gamma}{N}$$

where γ is the dimensionless 'shape factor' which only depends on the functional form of the excitation profile.

This property of $G(0)$ was initially tried in our original setup to determine concentrations. However, correlated noise inherent in the mechanical scanning device, as will be explained in the next chapter, was an obstacle not surmountable in an easy and inexpensive way. This prevented us from using the autocorrelation function for particle-counting purposes. One possible solution was to use optical confocal techniques combined with the Photon Counting Histogram (PCH) method.

The PCH Method

The analysis of time sequence of the fluorescence fluctuation is traditionally used to provide the number of fluorescent particles in the excitation volume and the autocorrelation time of the fluctuation through the analysis method of Fluorescence Correlation Spectroscopy (FCS), as discussed above. It has been recently demonstrated in our lab that Photon Counting Histogram (PCH) analysis constitutes a novel tool to extract quantities from fluorescence fluctuation data (Chen 1999; Chen, Muller et al. 1999). PCH characterizes the amplitude distribution of fluctuations of fluorescent light emanating from a small volume of the sample, that is, the probability distribution to detect a given number of photons per sampling time. For a single species of fluorescent particles, PCH is completely characterized by two parameters: the average number of particles in the observation volume, and the particle brightness, defined as the average number of detected photons per sampling time per particle.

The low light levels usually encountered in fluorescence experiments such as FCS require the use of photon counting techniques and efficient photon detectors such as avalanche photodiodes or photo-multiplier tubes. When a photon is absorbed by the detector, a charge separation is induced. This charge is subsequently amplified to yield an electronic signal. A semiclassical treatment of the detection process is adequate to cover most experimental situations (Saleh 1978). The probability of observing k photoelectron events at time t is given by Mandel's formula

$$p(k,t,T) = \int_0^\infty \frac{(\eta_W W)^k e^{-\eta_W W}}{k!} p(W)\,dW$$

η_W is the detection efficiency. The energy of light falling upon the detector surface is given by the light intensity $I(r,t)$ integrated over the time period T and detector area A,

$$W = \int_t^{t+T}\int_A I(r,t)\,dA\,dt$$

The distribution $p(k,t,T)$ is characterized by a variance $\langle \Delta k^2 \rangle$ which is greater than its mean value $\langle k \rangle$ and is thus classified as super-Poissonian. This is due to the fact that two sources of randomness are encountered: (1) Shot noise, a random Poissonian point process reflecting the discreteness and the independence of the photoelectric detection process , and (2) Fluctuations in the light intensity reaching the detector which is characterized by the probability distribution $p(W)$.

Experimentally, the effect of the microscope focusing optics and the detector on the shape of the observation volume is characterized by the point-spread function (PSF) of the instrument. The shape of the latter influences the photon count distribution. The

fluorescence intensity at the detector for a particle at position $\vec{r}$ is given by the PSF and the excitation intensity I_0 at the center of the PSF:

$$I = I_0 \beta PSF(\vec{r})$$

where the coefficient β contains the cumulative effect of the excitation probability, the fluorescence quantum yield, the quantum yield of the detector , and all the instrument-dependant factors, such as transmittance through the microscope optics.

It can be shown that the PCH for an open system is given by (Chen 1999; Chen, Muller et al. 1999)

$$\Pi(k;\overline{N},\varepsilon) = \sum_{N=0}^{\infty} p^{(N)}(k;V_0,\varepsilon)\widetilde{p}(N),$$

with

$$\widetilde{p}(N) = Poi(N,\overline{N})$$

where the average number of particles given by $\overline{N} = cV_0N_A$, c being the molar concentration of the solution and N_A Avogadro's number,

$$p^{(N)}(k;V_0,\varepsilon) = (\underbrace{p^{(1)} \otimes \cdots \otimes p^{(1)}}_{N \cdot factors})(k;V_0,\varepsilon),$$

$$p^{(1)}(k;V_0,\varepsilon) = \int Poi[k,\varepsilon PSF(\vec{r})]p(\vec{r})d\vec{r} = \frac{1}{V_0}\int_{V_0} Poi[k,\varepsilon PSF(\vec{r})d\vec{r}$$

is the probability for a single particle in volume V_0 that contains the PSF, and ε describes particle brightness and is deduced from the average photon counts given by $p^{(1)}$

$$\langle k \rangle = \frac{\varepsilon}{V_0}\int_{V_0} PSF(\vec{r})d\vec{r} = \varepsilon\frac{V_{PSF}}{V_0}.$$

A more intrinsic parameter independent of the sampling time would be $\varepsilon_0 = \varepsilon / T$; it expresses the particle brightness in photon counts per second per particle. However, this is still instrument-dependant.

As mentioned earlier, for a single species of fluorescent particles, PCH is completely characterized by two parameters: the average number of particles in the observation volume, and the particle brightness. In principle therefore, a technique based on PCH could be used to determine fluorescent particle concentration in fluid samples. In addition, the particle brightness, assuming a homogeneous sample could also be determined. This latter property being instrument-dependant, the intrinsic brightness could be deduced using a standard fluorophore sample, such as Fluorescein or Rhodamine. As a very useful practical expansion of the technique, it is possible, using a PCH analysis, to distinguish multiple species in a single sample run if they have well spaced brightness magnitudes.

A data analysis method based on the PCH technique was successfully applied for the determination of the Somatic Cell Count in raw milk, as shown in the next chapter.

Chapter 3 Experiments with Milk: Determination of Somatic Cell Count (SCC)

Outline

In this chapter I discuss a real life application and candidate for the instrument we built. The concept and importance of the determination of the somatic cell count (SCC) in milk for the dairy and related industries is briefly explained. This is followed by a discussion of the mechanical and optical components of our experimental setup. Calibration results with fluorospheres both in clear and turbid media using a variant of PCH are given. The same procedure is followed in the measurement of the SCC in fresh milk. A discussion of the possibilities and limitations of the method follows.

What is SCC?

Counting of cells in raw milk is such an important problem to the dairy industry. Mastitis is the most costly disease of dairy cattle. Estimates of the total losses for the U.S. are upward of 3.0 billion dollars annually (Harmon 2001). These economic losses are due to treatment, discarded milk, death and premature culling, and reduced milk production, with the last factor accounting for 70% of the total losses.

Mastitis is an inflammation of the udder or mammary gland. When bacteria enter the gland and establish an infection, the ensuing inflammation is accompanied by an influx of white blood cells from the blood stream. Milk somatic cells are primarily leukocytes, which include macrophages, lymphocytes, and neutrophils, with epithelial

cells from the udder tissue accounting for less than 7% of the total. Since cell counts in milk are closely associated with udder health, the somatic cell count (SCC) is accepted as an international standard measurement of milk quality. An SCC of $2x10^5$ /ml is usually considered to be the maximum for an animal to be considered free of Mastitis. Other thresholds are also critical for particular uses of milk such as in its suitability in making different kinds of cheese. Also SCC is an important indicator of subclinical Mastitis, the precursor of the full-blown clinical Mastitis. Subclinical Mastitis is harder to detect since there are no manifest symptoms in the cow or its milk to suggest a problem. For every case of Mastitis, there are usually two or three dozen cases of subclinical Mastitis across the herd. As a consequence, the best way to control losses is to recognize the disease before it spreads either in a given animal or across the herd (Cerrusi 1999; Harmon 2001).

There are a variety of tests available to estimate or determine the SCC. They range from the inexpensive but very imprecise, such as the California Mastitis Test (CMT), to the sophisticated and very expensive laboratory procedures, like the Direct Microscopic Somatic Cell Count (DMSCC).

The CMT test, for example, is conducted by mixing a test reagent containing a detergent with an equal quantity of milk. It reacts with the nucleic acids from somatic cells in the milk to form a gel. The reaction is then visually scored as 0, T (Trace), 1, 2, or 3, depending upon the amount of gel that forms. The more gel which forms, the higher the score. This indicates a higher number of somatic cells present. CMT scores correlate with average somatic cell concentrations as follows: CMT-0 = 100,000, CMT-T = 300,000, CMT-1 = 900,000, CMT-2 = 2,700,000 and CMT-3 = 8,100,000. Table 3.1

illustrates the approximate ranges in somatic cell concentrations associated with each of the CMT scores (Harmon 2001).

Score	Somatic Cell Range		
N	0	--	200,000
T	200,000	--	400,000
1	400,000	--	1,200,000
2	1,200,000	--	5,000,000
3	over 5,000,000		

Table 3.1 Approximate ranges in somatic cell counts for California Mastitis Test scores

Another widely used test, the Wisconsin Mastitis Test (WMT), is primarily a laboratory test and is generally conducted on bulk tank milk samples. The test is very similar to the CMT in that it uses the same type of reagent; however, the reaction is not estimated but is measured. This increases the objectivity of the test. However, the WMT requires more sophisticated equipment and more time than does the CMT procedure.

The Direct Microscopic Somatic Cell Count (DMSCC) is the most accurate of the mastitis screening tests when conducted properly. For this reason, regulatory agencies generally use this test for confirmation of high somatic cell counts based on other tests. DMSCC is also the standard by which all other tests are calibrated. It is however the most time consuming and requires expensive equipment.

Some SCC measurements are performed on bulk-tank milk, and an abnormal SCC would indicate problems in the herd as opposed to an individual cow. In addition, very few measurements distinguish between the quarters of a given cow. There is indeed a

need for an inexpensive, precise and simple on-the-farm procedure to determine the SCC of single quarters in individual animals (Cerrusi 1999; Harmon 2001).

Experimental Setup

The apparatus used in the experiments is entirely homemade (Fig. 3.1). It consists of a small microscope that has a horizontal geometry and a mechanical instrument that holds a cylindrical cuvette (1 cm in diameter) with two motors that provide a rotational and a vertical up-and-down motions. The rate of the rotational motion of the cuvette around its long axis was 5 Rev./sec for the experiments dealt with in this chapter. It was provided by a small synchronous direct motor rated at 300 RPM (Hurst Manufacturing, SA4001-001).The vertical motion along the axis of the cuvette was made slower to insure statistical independence of the illumination subvolumes explored in consecutive vertical scanning cycles. Statistically independent subvolumes refer to sample volumes that do not have the same composition due to diffusion and other transport processes affecting the particles in the sample. In our setup, the vertical motion was provided by another synchronous motor (Hurst Manufacturing, RA3905-001, 300 RPM) coupled to a micrometer. The latter was linked to a stage holding the cuvette and the other smaller motor providing the rotational motion (see Figure 3.2). The micrometer serves to convert the motor's rotational motion into a linear one for the stage and to make the vertical sweeps very slow, even though the motor providing the motion has a relatively high RPM. A combination of an electromagnetic relay and two switches with adjustable positions provide the reversing mechanism for the up-down vertical motion of the stage. The amount of vertical sweep can be varied by sliding the switch mounts. The

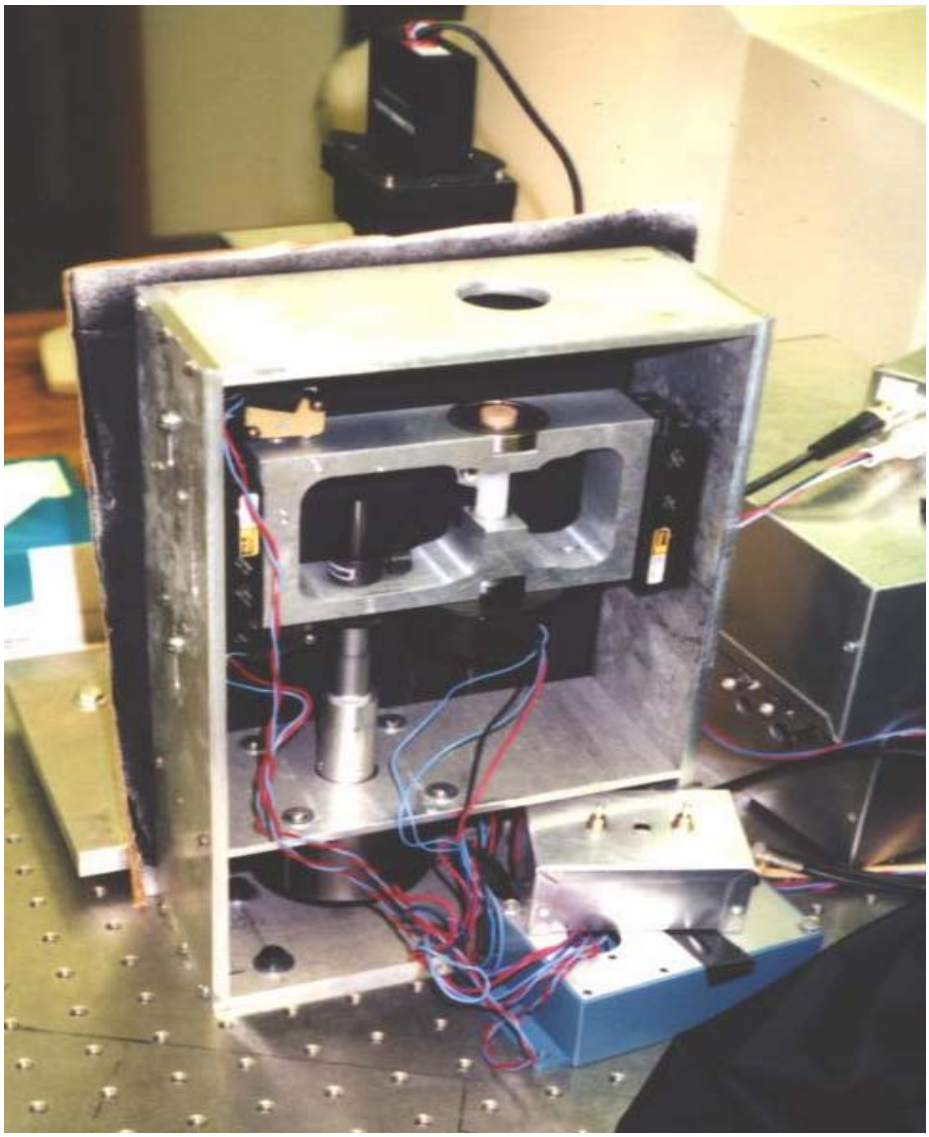

Figure 3.1 Photograph of the device used in the experiments

It is entirely homemade. It consists of a small confocal microscope that has a horizontal geometry and a mechanical instrument that holds a cylindrical cuvette (1 cm in diameter) with two motors that provide a rotational (5rev./sec) and vertical up-and-down (~2.5sec period) motions. The device looks like a simplified flow cytometer. The total volume that is explored is very large.

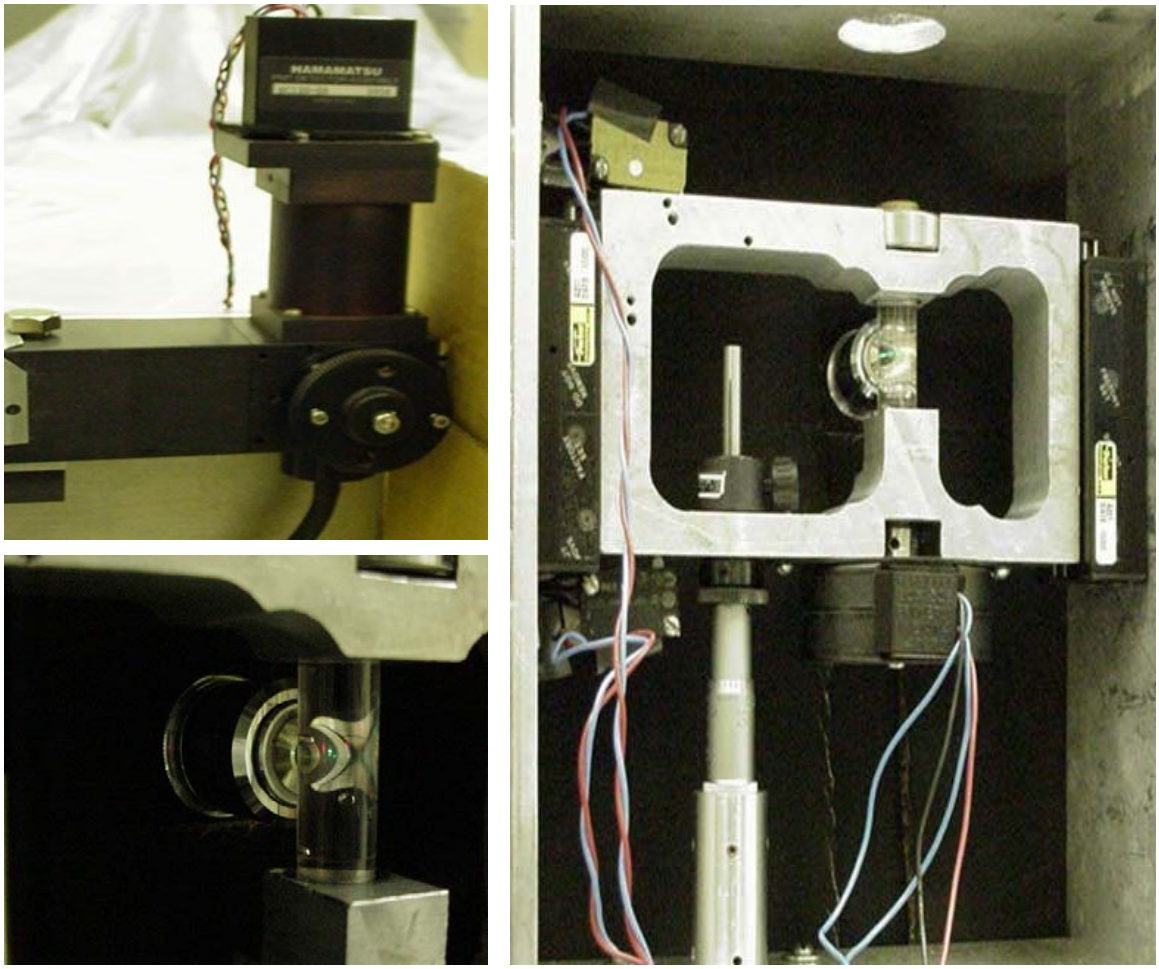

Figure 3.2 Details of the Apparatus

Upper left: The microscope. Excitation light comes from the left. The PMT is seen at the top to receive fluorescence emitted from the sample
Right: Mechanical setup. The stage holding the cylindrical cuvette in front of the objective of the microscope also holds the small motor providing rotational motion of cuvette. The micrometer on the left acts as the driveshaft for vertical motion provided by the other motor (below level of image, can be seen in fig. 1.)
Lower left: More detail of microscope objective and cylindrical cuvette that holds sample.

illumination focus was positioned relatively close to the wall of the container, at about 200 μm inside the cuvette. This feature insures that particle detection and analysis could be done even in highly scattering media.

Use of a confocal microscope in combination with a simple mechanical way for moving the sample container in front of the objective provides a means for transporting the sample containing particles through an observation region without requiring complex optical systems comprising moveable optical components, such as translating optical sources, mirrors, or photodetector. This aspect of the setup is advantageous as it provides a simple, mechanically robust experimental system that does not require repeated optical realignment between scans.

Figure 3.3 gives a schematic view of the whole experimental setup. For excitation source, we have used alternatively a halogen lamp coupled to a 525nm band-pass filter with FWHM of 60nm, an Argon ion laser (Stabilite 2017, Spectra-Physics) at 515nm excitation, and lately, a laser pointer at 532 nm excitation (Worldstar, DPGL-20). The output power needed is less than 1mW. The objective used is Kyowa 20x (N.A. 0.40). A long pass emission filter is used to eliminate the remaining excitation light left by the dichroic mirror (Chroma, Z532RDC). The dichroic mirror in our setup transmits excitation light and reflects fluorescence emitted from the sample. For fluorescence detection, a photo-multiplier tube (PMT) HC120 (Hamamatsu) is used throughout. The signal from the PMT is fed into a dual-channel DRA acquisition card. The photocurrent is digitized and sampled with a variable time resolution. For the experiments mentioned in this chapter, a sampling rate of 40 kHz was used. The time trace of the signal giving the photocurrent per time bin as a function of time is stored in the computer and analyzed

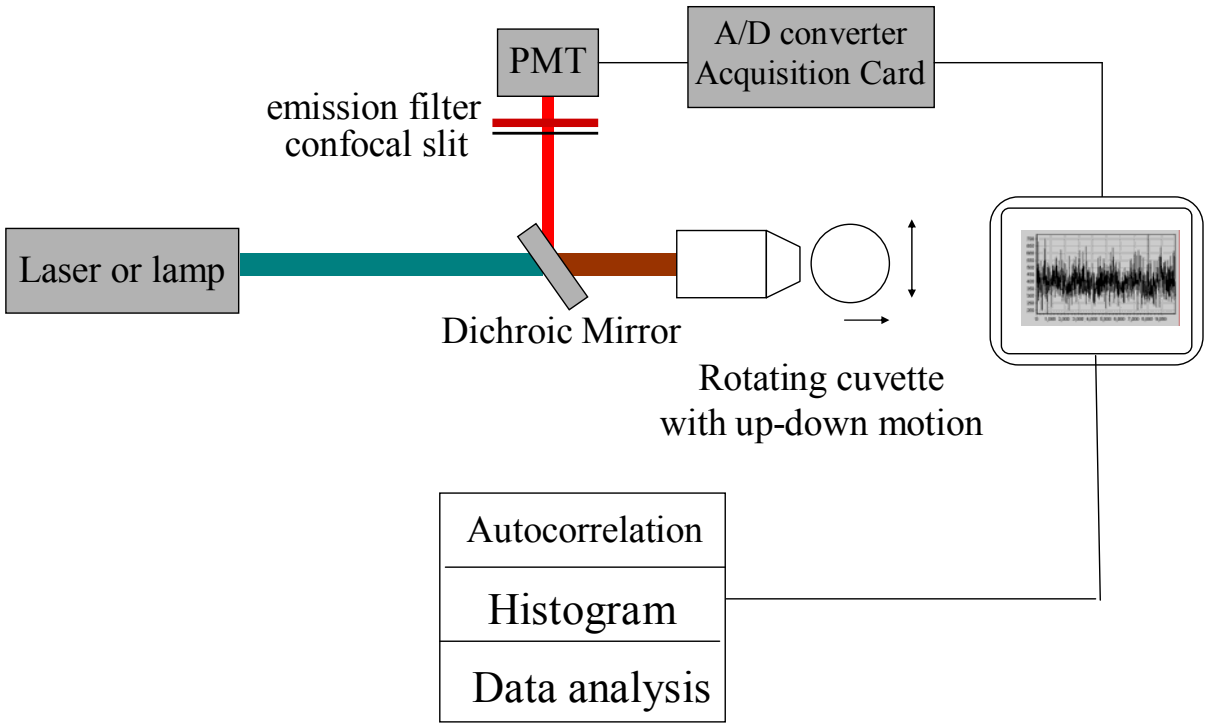

Figure 3.3 Schematic diagram of the experimental setup

Excitation light from laser or lamp is focused by microscope objective inside the cuvette holding the ample very close to its wall (bottom left). The cuvette is rotated and moved vertically perpendicular to the plane of the plane of the figure to scan the sample in a helical fashion. Emitted florescence collected by the same objective is reflected by the dichroic mirror and the signal amplified by the PMT. A confocal slit and an emission filter are placed in front of the PMT window. The output of the PMT is processed by an acquisition card and analyzed by the computer

using a comprehensive program software, simFCS, developed at our laboratory. Among many other functions, simFCS calculates the autocorrelation function and the photon counting histogram.

The volume of the PSF for the confocal setup used in the following experiments was estimated as follows:

$$V_{PSF} \approx L_x L_y L_z$$

When a rectangular slit is used in front of the photodetector, L_x and L_y correspond to axes that are orthogonal to the propagation axis of the excitation light and are calculated using the physical dimensions of the slit and the magnification factor of the confocal microscope, and L_z corresponds to an axis parallel to the propagation axis of the excitation light (optical axis) and is estimated using physical optics. In the embodiment used here to detect and count fluorospheres,

$$V_{PSF} \approx 70\mu m \cdot 500\mu m \cdot 150\mu m \approx 5 \cdot 10^6 \mu m^3$$

The total length of the trajectory for a measurement time t is

$$L = \pi D \omega t$$

$D = 1cm$ being the diameter of the cuvette and $\omega = 5rev/s$ is the angular speed of rotation. This gives, for a total scanning time of 100 seconds,

$$L \approx 1.6 \cdot 10^7 \mu m$$

So that the corresponding total volume explored, given by the product of the cross section $L_y L_z$ by the trajectory length L, is

$$V_{tot} \approx 500\mu m \cdot 150\mu m \cdot 1.6 \cdot 10^7 \mu m \approx 1.2 \cdot 10^{12} \mu m^3 = 1.2ml$$

Therefore, more than 1 ml of volume is explored during a 100-sec measurement time in this experimental configuration. This calculation illustrates the potential of the device to detect very low concentrations (a few per milliliter) in reasonably short scanning times.

It is important to note that the sample fluid never "enters" the inner workings of the device. Careful filtering is not necessary to prevent clogging. Frequent cleaning is not needed to prevent contamination or bacterial growth. The sample is also not lost as in flow cytometry. It remains in the cuvette and, thus, can be subjected to other tests if desired. This attribute of the present instrument is a significant advantage when working with hard-to-get samples.

Calibration with Fluorescent Spheres in Clear and Turbid Media

We initially worked with orange fluorescent spheres, 1.0 μm in diameter (Molecular Probes, F-8820) in both a clear buffered solution and a Lyposin solution (20% weight diluted 1:80, Scattering sample). We used a small halogen lamp combined with a green filter (525±60nm). A longpass filter (threshold at about 590 nm) was used at emission in front of PMT. We were able with this method to get resolutions down to a few thousand/ml in one-minute scanning time. Figure 3.4 shows photon current histograms as a function of particle concentrations. The broadening of the histogram clearly depends on the concentration of fluorescent particles in the sample. Rather than doing complex fittings as in regular one-molecule PCH procedure, we simply set a threshold, to eliminate most of the contribution from the background noise, and added the photon current counts above this threshold. What we obtained was the calibration curve

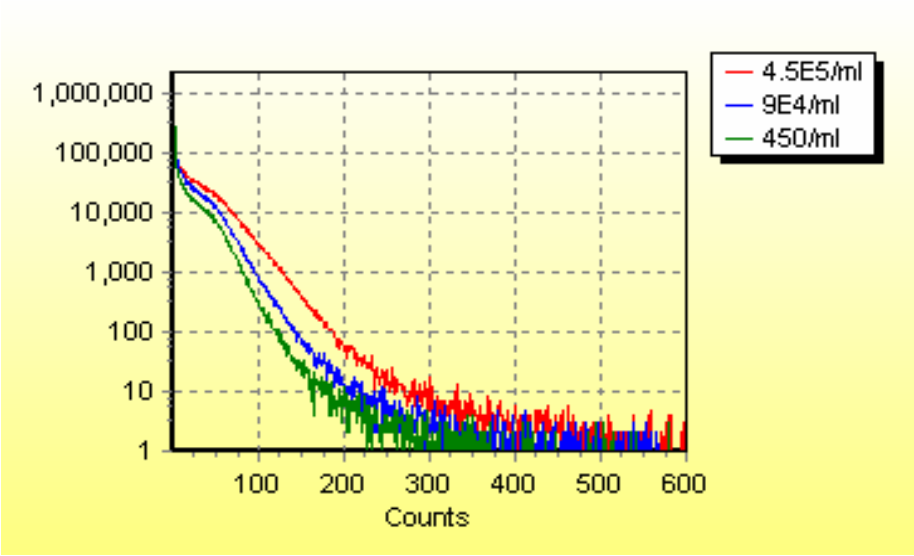

Figure 3.4 Representatives of current histograms for different concentrations of spheres

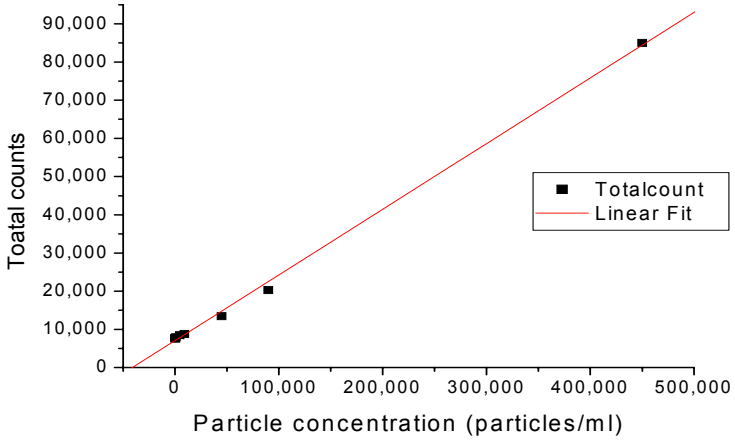

Figure 3.5 Total counts (from a threshold) versus particle concentration. The linearity is good over a wide range of concentrations

shown in figure 3.5. The linearity of the curve is not too sensitive to the choice of the threshold. There is a very good linear fit over a wide range of concentrations.

Measurement of Somatic Cell Count in Milk

Fresh raw milk was obtained from the dairy cattle research unit on campus. The milk was diluted to 1/4 in TRIS buffer. We started with milk from a cow that was being treated for Mastitis. Her SCC was around 1,000,000 cells/ml. Ten dilutions were done to cover the useful range of SCC (10^5 - 10^6 cells/ml). A solution of Lyposin at 0.25% concentration was substituted for milk to keep the same level of scattering in the dilutions. A detergent (Triton-X 100) was added to compromise the cell membranes. Finally, Ethidium bromide (Molecular Probes, E-1305) was added at a concentration of 10 μM to tag the cells. Ethidium bromide associates with the DNA in the nuclei of the cells where its fluorescence is enhanced by a factor of about twenty over that of its free form.

Figure 3.6 shows an exemplary photon current histogram generated by the present methods for a milk sample containing somatic cells. The broadening of the histogram in the figure shows a dependence on the concentration of fluorescent particles in the sample. To generate a useful calibration curve for this system, a fluorescence intensity threshold was set as was done above with the fluorospheres. Figure 3.7 shows a plot of total counts (peaks in the fluorescence temporal profile about the threshold) as a function of somatic cell concentrations generated using the present method and device. As shown in the

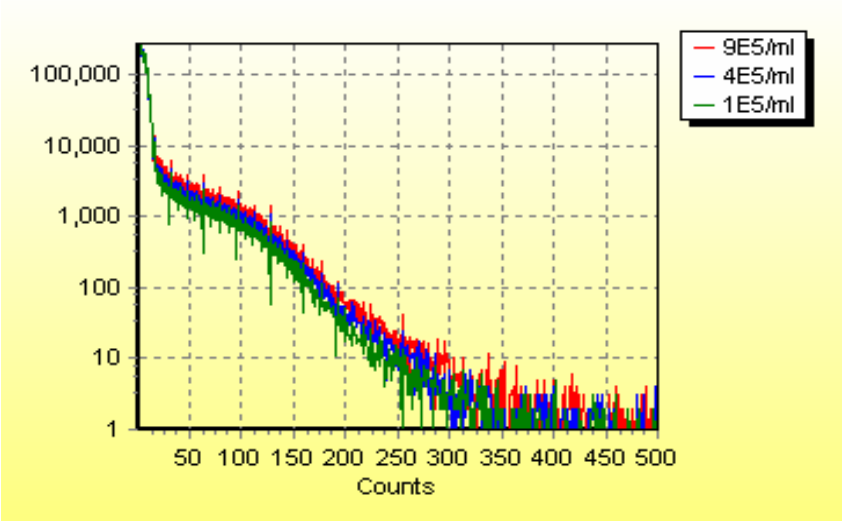

Figure 3.6 Histograms for different cell counts in milk

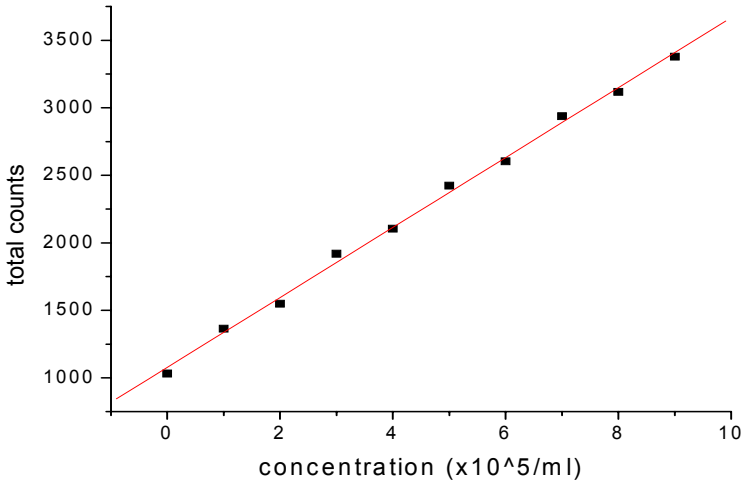

Figure 3.7 Measurement of somatic cell count in milk

figure, there is a very good linear fit over the useful range of concentrations examined. Furthermore, repeated analysis of the raw data indicated that the linearity of the calibration curve is not very sensitive to the choice of the fluorescence intensity threshold.

Discussion

The use of this modified, PCH-based method on our instrument gave adequate results for large concentrations. Measuring the SCC, for example, dealt with cells upward of $2.5x10^4$/ml (10^5/ml x ¼ TRIS buffer dilution). The method involved subtracting most of the contribution of the background by summing current intensities starting from a threshold. This maneuver did not present us with problems for large concentrations as the relation between intensity current sums and concentrations remained linear, largely independent of the choice of intensity threshold. This shortcoming could be handled in practical applications of the method by the use of an appropriately prepared sample that would serve for an initial calibration of the system. For example the standard sample could be prepared by using a known concentration of fluorospheres in a fluid that could be turned into a gel inside a cuvette. That would make maintaining the standard sample easier and its lifetime longer. Many parameters could then be adjusted as to give the same result for the standard each time it is used. These include excitation power, PMT voltage level, and photon intensity current threshold.

Calibration intricacies aside, problems arose when we wanted to measure turbid samples with concentrations lower than 10,000/ml. The linearity of the curve was lost as the particle concentration was lowered. Additionally, there was no correlation between

photon current intensities and particle concentration at very low values of the latter. Worse, results were not consistent and lacked repeatability for the same sample, especially when cuvettes where changed. The reason for these problems is that the photon counting histogram includes contributions from the background and effects of the mechanical rotation in addition to the signal from the particles of interest, as figure 3.8 sows. All cuvettes are not made the same, and simply changing the cuvette presents the system with a different scattering profile. The relative contribution of this background increases as the contribution of the signal from the fluorescent particles decreases with decreasing concentrations. Simple data filtering, such as low-pass to handle the baseline signal modulations brought about by the rotation of the cuvette, was not enough to achieve our goal of conquering low concentrations. The problem is especially more pronounced when dealing with faint particles in a scattering medium. In our push to reproducibly detect and measure even lower concentrations, a correlation filter program based on pattern recognition was written. The new program recognizes the passage of each particle of interest in the illumination volume during the scanning, records the event as a hit along with its intensity amplitude. This is the subject of the next chapter.

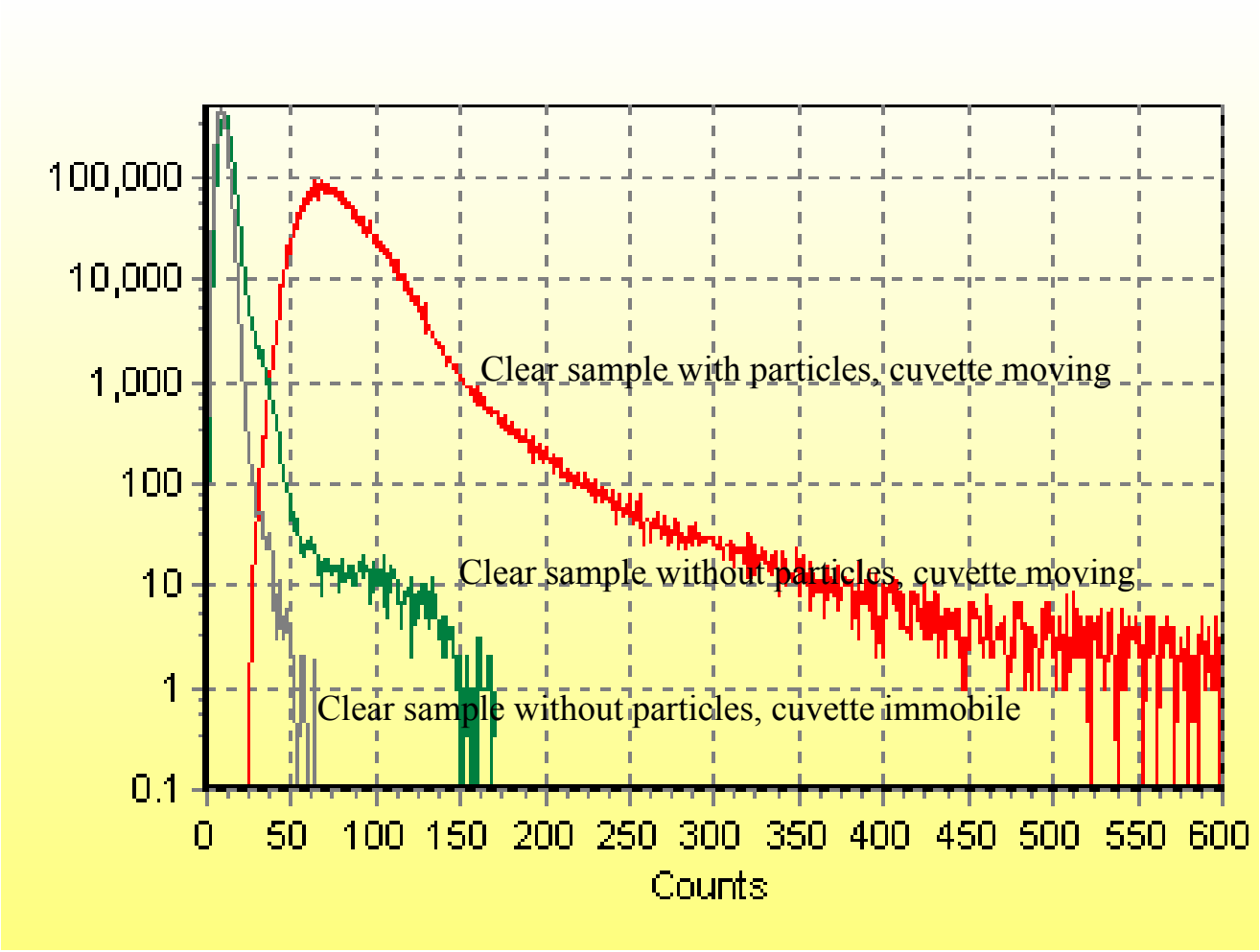

Figure 3.8 Effect of cuvette motion on histogram

Chapter 4 Advanced Setup with Data Filtration

Outline

This chapter begins with a motivation for the new method of data filtration for the detection of fluorescently-tagged particles in fluids. I introduce this program that enabled us to reach detection in the attomolar range in reasonably short times. I describe how the pattern–recognition based algorithms work and discuss their advantages and the many obstacles they helped us conquer.

Introduction

From the results of the last chapter, it is very clear that the conventional point-FCS or PCH cannot be applied to very dilute samples, i.e. samples with concentration of fluorescent particles well below the picomolar. On the other hand, the samples of interest to us, cells and aggregates with potentially very many fluorescent molecules associated with them, are relatively much brighter than normally dealt with in conventional FCS experiments. However, the presence of the cells in the laser focus was very rare. After considering many options, we opted to keep the mechanical and optical setup as it is, for we have shown, as evident from the last chapter, that using a combination of mechanical rotation and vertical cyclic translation, coupled with an optical confocal setup, the total volume explored in a reasonably short time is very large (~ 1 ml/min). The goal, as decided from the outset, was to keep the device and technique simple yet powerful and ultimately inexpensive and portable. The solution would have to be a data analysis

technique that would provide for a much better way of discriminating the passage of a particle from the other noises in the system. In antibody-based assays for example, there is always a relatively large quantity of free fluorescent material. In our technique, what is important is the ratio of the number of fluorophores on the particle with respect to the free fluorophores. However, there are several factors that help the detection of a burst of fluorescence even in the presence of relatively large uniform background in addition to reducing the observation volume, as shown in figure 4.1. For example, if we know the shape of the burst then we can test the system for specific burst patterns. This way, we will be counting only particles that pass through the observation volume that are of interest of us, and then deducing concentrations. The same concept of 'pattern recognition' is also used to detect the length of the burst for particle size determination, as will be considered in a later chapter. Combination of the large volume of exploration, the regular motion of the sample and the pattern recognition algorithm, resulted in unprecedented sensitivity for the detection of a small number of particles in a relatively large volume as explained in this chapter and shown in the next.

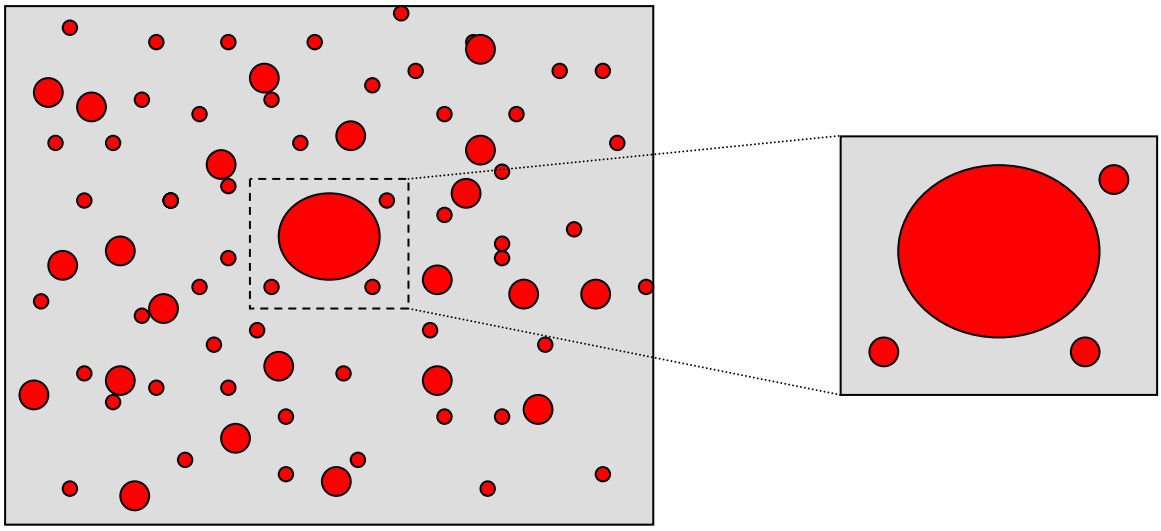

Figure 4.1 Decreasing the volume of observation results in larger signal-to-noise ratio

Pattern-Recognition Based Filter

The pattern recognition program analyzes the temporal profile of the digitized signal from the detector to determine the concentration of particles in the sample. The pattern recognition algorithms match features in the temporal profile to a predetermined pattern that correspond to the time-dependent fluorescence intensities of particles passing through the observation volume. Figure 4.2 shows the time trace from particles passing through the excitation volume. Predetermined patterns useful in the present setup comprise a distribution of intensities as a function of time, and may be determined

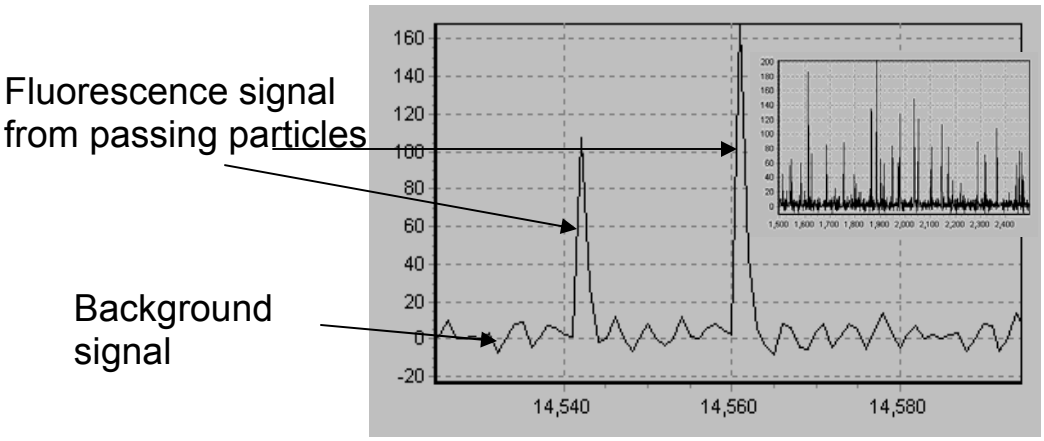

Figure 4.2 time trace of fluorescence signal from particles passing through observation volume.
Inset: long-time trace of signal

empirically or calculated *ab initio*, taking into account the shape of the point spread function (PSF) of the optical setup, the speed of the particles, and the rate of signal sampling.

Discrete particle detection events are identified by establishing a match between the amplitude and shape of a feature in the temporal profile and the predetermined pattern. The concentration of particles is determined by calculating the number of predetermined patterns matched to features in the temporal profile for a given sample scanning period. In the experiments that follow, this matching is performed by operation of a filter algorithm that performs a least squares calculation at each point of the huge vector, representing the fluorescence detected as a function of time. The program calculates the best amplitude of the filter that minimizes the local Chi square, the intensity amplitude not being restricted. The Chi square is calculated by weighting the difference between the raw data and the fit to the predetermined pattern with the sum of the noise level specified in the noise window and an estimation of the standard deviation

that accounts for the square root of the number of counts at the particular point of the huge vector representing the total fluorescence signal intensity as a function of time.

Figure 4.3A shows a temporal profile (top plot) generated by the optical analyzer and corresponding predetermined patterns (middle plot) matched to features in the temporal profile. Also shown in Figure 4.3A are the Chi square values (bottom plot) associated with each pattern matched to the temporal profile. Figure 4.3B provides an overlap plot showing a feature observed in a temporal profile and a predetermined pattern fit to match the feature. The program is written so that individual matches can be separately viewed. Figure 4.3C shows the intensity distribution for the particles in the sample.

Concentrations are extracted from the analyzed temporal profile by dividing the number of matches by the total volume of sample analyzed during a selected sample scanning period, which can be accurately calculated with knowledge of the size of the observation volume, rate of movement of the cuvette (rotational) and the duration of the sample scanning period. The size of the observation volume is controlled by the size of the confocal aperture employed in the confocal microscope. Smaller observation volumes are beneficial for increasing the signal-to-background ratio and ensuring that particles pass through the observation volume and are detected one at time, especially when dealing with high particle concentrations. Use of smaller observation volumes, on the other hand, requires longer sample scanning periods, especially in the case of very low concentrations. Accordingly, selection of the observation volume and sample scanning time represents a trade off in device performance attributes. In most applications, the

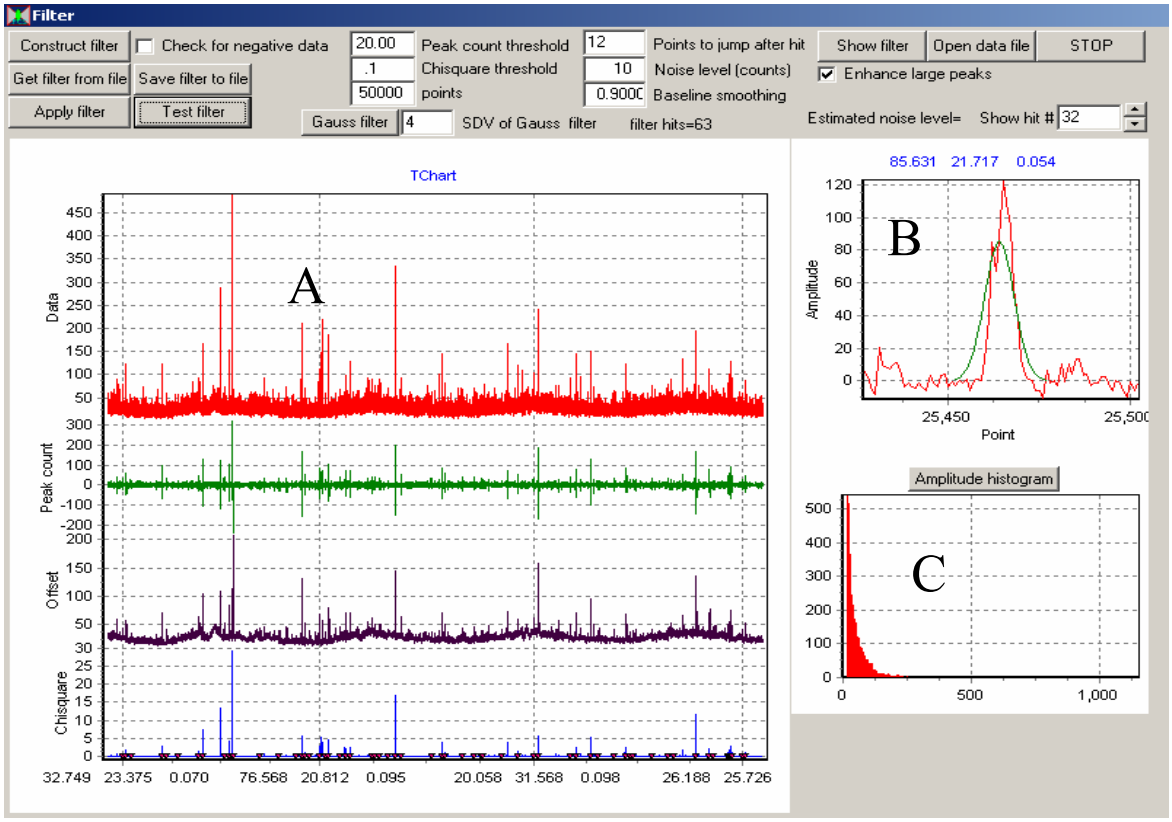

Figure 4.3 Interface of the filtration software as used in this chapter. The top part shows user-adjustable parameters

A: Temporal profile of the data collected (top)
Peak count and offset from varying background noise
Chisquare values of peaks

B: shows an example of a match between basic pattern (here a Gaussian) and temporal profile of passage of a particle

C: Intensity amplitude histogram of particles detected

best compromise is to use the largest confocal aperture that provides accurate detection and characterization of the particles of interest. By increasing the observation volume (using a wider confocal aperture), the total volume scanned for a given run time is larger. Alternatively, samples undergoing optical analysis may be diluted prior to analysis to achieve a concentration that ensures that particles are transported one at a time through a detection volume having a selected size. Sample dilution may also be useful when characterizing particles dispersed in highly scattering or absorbing media.

The total volume of sample analyzed during a given scanning period can also be determined empirically by the use of a standard. A sample of fluorophores of known concentration could be used to deduce the volume of sample scanned in say one minute. The total volume being directly proportional to the time of scanning, the corresponding volume for any other duration can be accurately determined, and thus particle concentration for any sample calculated.

Advantages of the Filtration Software

Use of the pattern recognition algorithms for the analysis of fluorescence data has been very beneficial because it enhances the sensitivity and expands the functional capability of the device. It allows for the detection of particles having low brightness at subattomolar concentrations (less than 10 particles per milliliter) using short sample scanning periods (of the order of a minute). This provides a huge improvement in sensitivity, about a factor of 10^8 compared to conventional scanning confocal microscopy methods. For example, a convective-diffusion-based FCS system to detect E. coli bacteria yielded a lower limit concentration of $5x10^5$ /ml using 20-minute long measurement periods (Qing, Menguc et al. 2003).

Another advantage of this data analysis approach is that the predetermined patterns useful for analysis via pattern recognition and their use in such analysis algorithms do not strongly depend on particle composition or the composition of the medium that the particles are dispersed in. The shape of the basic pattern is determined by the flow and the geometry of the Point Spread Function, not the nature of the particle or the medium. In the present setup, concentration measurements involve identifying the number of particle detection events and a determination of the net volume of sample scanned during a sample scanning period. Particle detection events are identified by matching the basic pattern to features in the observed temporal profile of fluorescence from an observation volume. Therefore, the present techniques permit the determination of the concentration of particles without elaborate calibration procedures strongly dependent on the precise nature of the system undergoing analysis.

Yet another major problem was solved with the application of the correlation filter algorithms. It was mentioned in the last chapter and has to do with the modulation of the baseline signal due to the mechanical rotation of the cuvette. Small precessions in this motion lead to the background varying with the orientation of the cuvette. The filtration algorithms take this into consideration. The matching of the basic pattern template is done locally, regardless of the level of the baseline intensity at that point. Setting a fluorescence intensity threshold is not sufficient as it would miss particles as figure 4.4 shows. This has made a tremendous difference to us, as it was extremely hard to completely get rid of the slight precession in the cuvette rotation. The filtration program made it unnecessary to have recourse to very expensive professional machining

for the mechanical setup of our device. This has an obvious positive effect on the ultimate cost of commercial machines based on our methods.

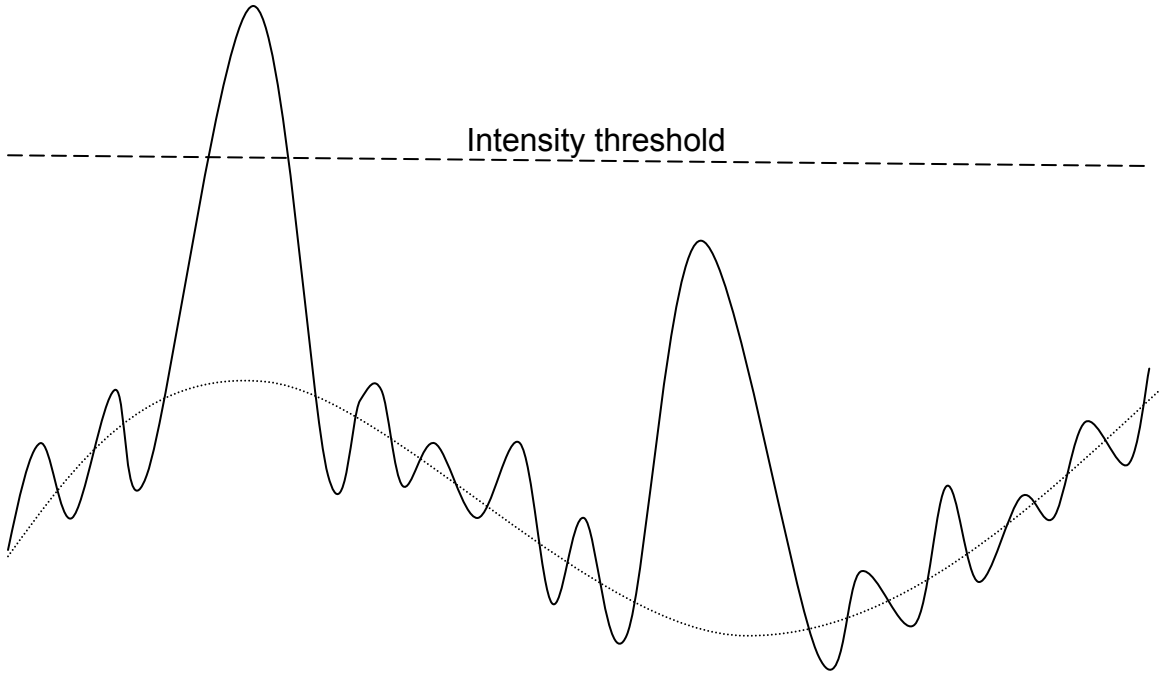

Figure 4.4 With the background fluorescence changing with time, setting an intensity threshold would miss many particle events

The next chapter gives examples of experimental results with different sample systems obtained using the instrument and this novel filtration analysis.

Chapter 5 Experimental Results Using the Correlation Filter Software

Outline

In this chapter I present experimental results obtained with the setup described in Chapter 3 and the correlation filter introduced in the last one. A biotechnological application very important to the food industry and which deals with the detection of trace amounts of virulent bacteria in food matrices using fluorescently-tagged antibodies is given and experimental results presented. This is followed by a discussion of the usefulness of the setup and the detection technique.

Fluorescent spheres

In our push to reproducibly detect and measure even lower concentrations (few particles per ml), a correlation filter program based on pattern recognition was written as described in the last chapter. The new program recognizes the passage of the particle of interest in the illumination volume during scanning, records the event as a hit along with its associated intensity amplitude.

To evaluate the effectiveness of the pattern recognition algorithms, an instrument calibration was performed using 1μm-diameter orange fluorescent spheres (Molecular Probes, F-8820). The experimental setup is similar to that of Chapter 3. For excitation source, we used a small laser pointer emitting at 532 nm with a rated power of 20 mW (WorldStar, DPGL-20). The laser unit was coupled to the microscope via a fiber optic

(3M, FT-400-EMT). The laser power at the microscope was less than 1 mW. At the emission side we used a bandpass filter (Chroma, HQ570/40M). The signal from the PMT was fed into a dual-channel DRA acquisition card. For the experiments mentioned in this chapter, the photocurrent was sampled at a rate of 60 kHz. The time trace of the signal giving the photocurrent per time bin as a function of time was stored in the computer and analyzed with the filtration software described in the last chapter and which was a new addition to simFCS mentioned earlier.

Figure 5.1 shows the result of a concentration-dilution study using the present optical analysis device employing pattern recognition data analysis. There is an excellent linear correlation between the total number of events as detected by the digital correlation filter and the actual concentration of fluorospheres in the samples. This linear relationship is maintained up to relatively high particle concentrations.

A very noticeable feature of the figure, however, is that starting at a certain high concentration threshold, there is a saturation of the number of events (particles) detected as the concentration increases. This is an expected result since at high concentration the probability of the simultaneous presence of more than one particle in the volume of observation increases. This concentration threshold is roughly equal to that corresponding to one particle per observation volume, i.e.

$$C_{thresh} \cong 1/V_{PSF}$$

To correct for the saturation effect, however, is straightforward. It could be accomplished by decreasing the volume of observation by changing the slit size in the emission side to a smaller one, performing a linearization of the curve taking into account the pile-up probability, or by simply diluting the sample prior to optical analysis.

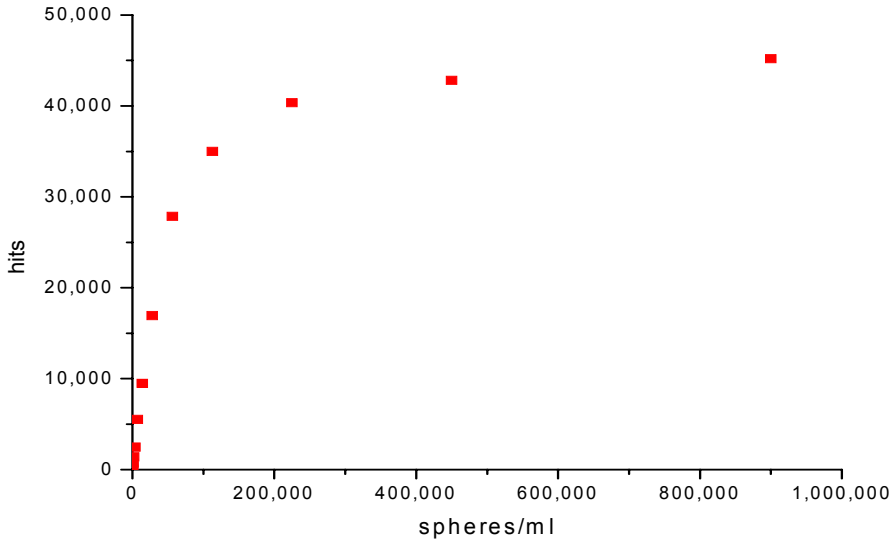

Figure 5.1 Calibration of fluorospheres using the filtration algorithms. A saturation is observed at very high concentrations

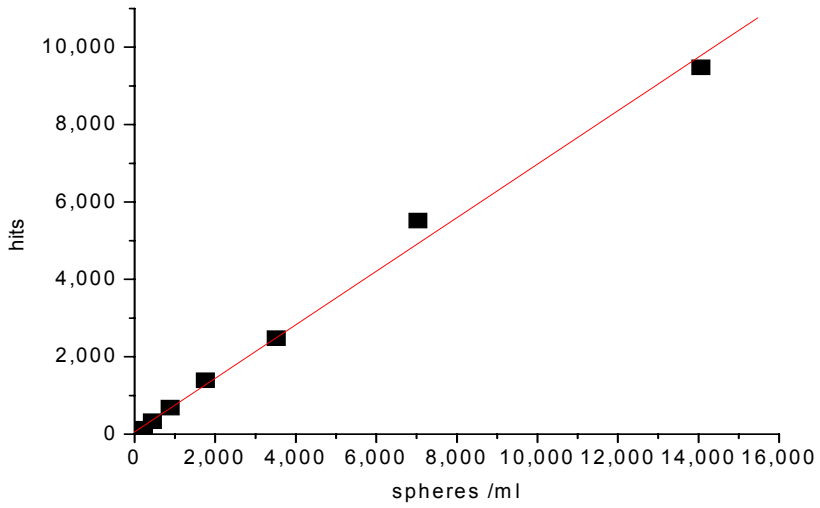

Figure 5.2 Linearity of the curve above at low concentrations is maintained to few spheres per ml.

In the low concentration part of the curve, and over a long range of concentrations, no correction for saturation effects is needed. In this regime, the linearity is excellent down to very low concentrations (few per ml), as shown in the figure 5.2. For these measurements, a scanning time of one minute was employed.

Results with E. coli bacteria

The ability of the present setup and filtration algorithms to measure the concentration of microorganisms, such as bacteria, was verified. In these experiments, E. coli bacteria were left to multiply for several hours in Luria Broth (LB) at a temperature of 37ºC and 300 rotations-per-minute agitation in an Incubator Shaker (New Brunswick Scientific, C24). A MOPS buffer solution was then used for sample dilutions. The bacteria were tagged with Sytox Orange (Molecular Probes, S-11368), a nucleic acid probe.

Figure 5.3 shows that the calibration performed with the fluorospheres holds for the much dimmer bacteria. Concentrations in the x-axis were estimated from plate counting done on the highest concentration, the others deduced from the dilution factors. Concentrations well below 100 per milliliter were measured employing a 1-minute scanning times. In addition, the software used for data analysis also performs an intensity analysis on all the particles detected. Figure 5.4 provides an amplitude histogram (i.e. intensity distribution). This demonstrates the ability of the present methods to classify particles based on their intensity distribution in mixed samples.

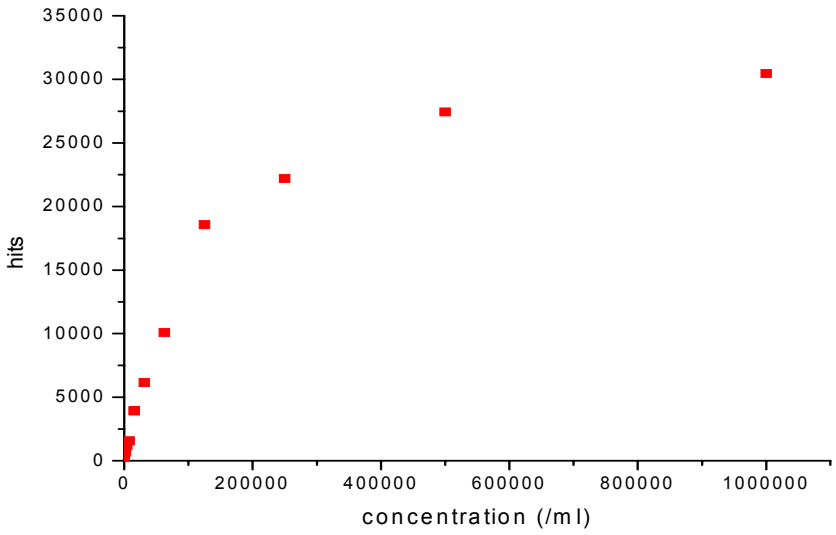

Figure 5.3 Calibration of E. coli bacteria using correlation filter

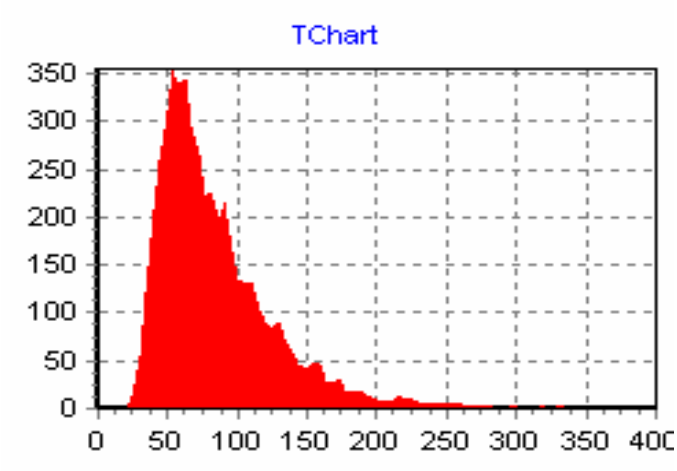

Figure 5.4 Amplitude histogram of positive hits for E. coli

Detection of *Salmonella typhimurium* in Food Matrices

A collaboration with Kim Laboratories in Champaign, IL to detect trace amounts of virulent microorganisms, such as *Salmonella typhimurium*, in diverse food matrices using tagged antibodies specific to the pathogen and no enrichment steps, provided a clear test and an actual biotechnological application of our instrument and techniques. Conventional testing methods for the detection of pathogens in food involve growth in pre-enrichment medium, followed by growth on selective medium and a battery of confirmatory biochemical and serological tests (Farber and Peterkin 1991). These methods are labor-intensive and time-consuming, often taking up to 10 days.

In many countries of the world, bacterial food-borne zoonotic infections are the most common cause of human intestinal diseases. Salmonella and Campylobacter account for over 90% of all reported cases of bacteria-related food poisoning world-wide (Thorns 2000).

Salmonella is a genus of Gram-negative rod-shaped bacteria from the enterics family that can cause diarrheal illness in humans (Jay 1992; Black 1996). Salmonella serotypes *Typhimurium* and *Enteritidis* are the most common ones in the United States. Salmonellosis is the clinical term for the infection caused by Salmonella. Most persons infected with Salmonella develop diarrhea, fever, and abdominal cramps 12 to 72 hours after infection. The illness usually lasts 4 to 7 days, and most persons recover without treatment. However, in some persons the diarrhea may be so severe that the patient needs to be hospitalized.

Every year, 40,000 to 50,000 cases of salmonellosis are reported in the United States. Because many milder cases are not diagnosed or reported, the actual number of

infections is much higher. It is estimated to be 2 to 4 million. Young children, the elderly, and the immunocompromised are the most likely to have severe infections. It is estimated that at least 500 persons die each year in the United States from acute Salmonellosis (Tortora, Funke et al. 1998).

Salmonella are usually transmitted to humans by eating contaminated foods. These foods are often of animal origin, such as beef, poultry, milk, or eggs, but all foods, including vegetables, may become contaminated. According to the United States Department of Agriculture (USDA), estimates of medical costs and losses in productivity due to food poisoning are up to $34.9 annually (Mead, Slutsker et al. 1999).

In our experiments, samples of ground beef and chicken breast were mixed with physiological saline and homogenized in a stomacher for several minutes prior to inoculation with Salmonella. *Salmonella typhimurium* (ATCC #14028) was grown in 5 ml of LB media overnight at 37 °C. The culture was washed and centrifuged in 0.1 M PBS buffer at pH 7.0 twice at 8000g (Eppendorf microcentrifuge 5415C) for 10 minutes. Cell pellet was reconstituted to its original concentration in PBS. Assuming overnight culture is in the standard concentration of $5x10^9$ cells/ml, $3x10^8$ Salmonella were aliquoted and reacted with 2.5 µg/ml of anti-Salmonella polyclonal antibody (CSA-1 by KPL Inc., catalog #01-91-99) labeled with Alexa Fluor 532 (Molecular Probes). The resulting reaction was incubated at room temperature for 20 minutes followed by centrifugation at 14,000 rpm for 10 min. The supernatant was removed and the cell pellet was resuspended in PBS. This washing step was performed once more. The pellet was then reconstituted to 1ml PBS and serially diluted until the final dilution had an MPC (most probable count) of 1 cell/ml. A portion of each diluted sample was plated on LB

agar and left overnight at 37 ºC to verify the concentration of actual CFU (colony forming units) /ml. Each dilution was measured with our instrument and the number of hits was correlated to the number of actual CFU/ml obtained by spread plating on LB agar after the reading.

We then evaluated the ability of the method to quantify *S. typhimurium* organisms in the meat matrices. Figure 5.5 shows the results of the measurements. The concentrations in the horizontal axis are determined from colony formation after a 24-hour incubation period in Petri dish.

The bacterial number and fluorescence emission were very well correlated in the bacterial concentration range from below 10 CFU/ml up to 10^6 CFU/ml. The capability of the instrument was remarkable in that its detection sensitivity was as low as few CFU/ml and yet its correlation consistent throughout a wide range of bacterial concentration. This indicates that the instrument can be used to detect bacteria in real time without the need of enrichment. In addition, it has a remarkable capability of cell enumeration providing valuable information to the end users.

Discussion

Our preliminary results indicate the possibility of a low-cost, portable instrument to detect and measure very low concentrations of particles in solution. The total data gathering time for the experiments mentioned in this chapter was short (~ 1-2 min.). 4-ml samples are used in this prototype. The S/N appears to be the only constraint for the detection limit of the concentration of particles that can be measured.

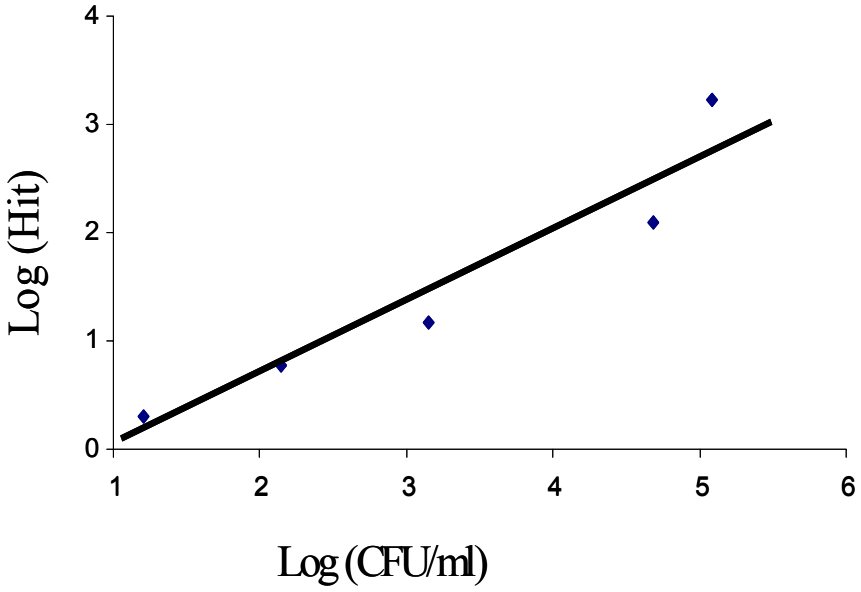

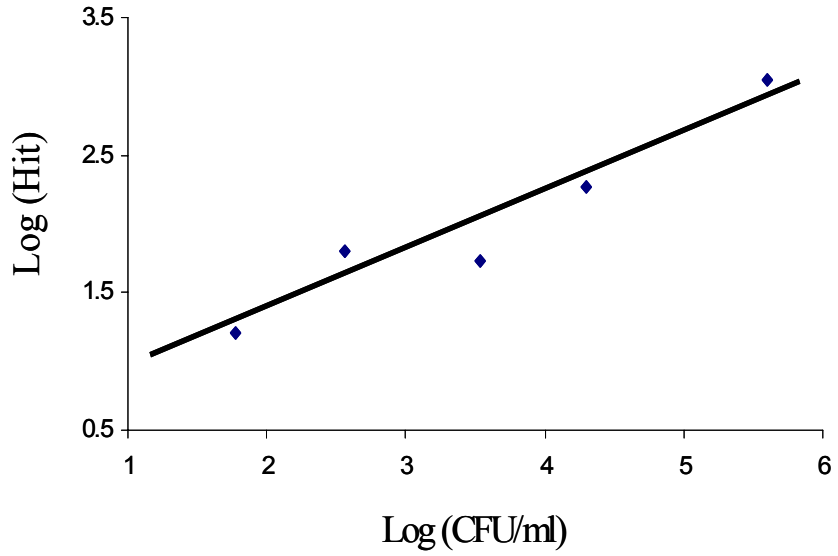

Figure 5.5 Results of measurements done with chicken breast above and ground beef below, spiked with *Salmonella typhimurium.* Commercial polyclonal antibodies specific to the microorganism were tagged with Alexa Fluor 532. Numbers in the x-axis were obtained through spread plating on LB agar. CFU=colony forming units

We have shown that at low concentrations, there is a linear relationship between the number of positive events and the concentration of particles. This proportionality is lost at higher concentrations. This is due to the increased probability of the detection of more than one particle in the observation volume at one time. Depending on the time lag between the arrivals of theses particles in the observation volume, this event is detected as a single particle of larger size and brightness, or simply ignored in the case of a longer time separation. Consequently, the linearity is maintained up to the concentration corresponding to one particle per observation volume. To remedy this non-linearity for high concentrations is straightforward as explained above. However, we are more interested in the more difficult problem of detection of trace amounts of particles.

A major advantage of the data analysis approach is that the predetermined patterns useful for analysis via pattern recognition and their use in such analysis algorithms do not strongly depend on particle composition or the composition of the medium that the particles are dispersed in. In the present setup, concentration measurements involve identifying the number of particle detection events and a determination of the net volume of sample scanned during a sample scanning period. Particle detection events are identified by matching a predetermined pattern to a feature in the observed temporal profile of fluorescence from an observation volume. Therefore, the present techniques permit the determination of the concentration of particles without elaborate calibration procedures strongly dependent on the precise nature of the system undergoing analysis.

Concentrations are extracted from the analyzed temporal profile by dividing the number of matches by the total volume of sample analyzed during a selected sample

scanning period, which can be calculated using the physical parameters of the mechanical and optical setup, or empirically deduced using a standard, as explained in chapter 4. The size of the observation volume is controlled by the size of the confocal aperture employed in the confocal microscope. Smaller observation volumes are beneficial for increasing the signal-to-background ratio, as shown in figure 5.6, and ensuring that particles pass through the observation volume and are detected one at time, especially when dealing with high particle concentrations. Use of smaller observation volumes, on the other hand, requires longer sample scanning periods, especially in the case of very low concentrations. Accordingly, selection of the observation volume and sample scanning time represents a trade off in device performance attributes. In most applications, the best compromise is to use the largest confocal aperture that provides accurate detection and characterization of the particles of interest. By increasing the observation volume (using a wider confocal aperture), the total volume scanned for a given run time is larger. Alternatively, samples undergoing optical analysis may be diluted prior to analysis to achieve a concentration that ensures that particles are transported one at a time through a detection volume having a selected size. Sample dilution may also be useful when characterizing particles dispersed in highly scattering or absorbing media.

For the detection of microorganisms, unlike many solid-phases immunoassays where conformational epitopes are often altered and antibody-binding hindered, a liquid medium as used in our setup allows for an unobstructed interaction between surface antigens and antigen-specific antibody. Our instrument is capable of detecting pathogens in turbid liquid samples as shown with measurements with milk and food matrices, making sample preparation and handling easier. Antibody-recognition and binding to

surface antigens labels healthy as well as stressed and injured bacteria since all express surface antigens abundantly.

It is important to stress that our detection system's capability is not limited by the type of microorganism detected, but by the availability of pathogen-specific antibodies. Therefore end-users will be able to utilize the same setup for a broad range of pathogen detection. Other clinical pathogens unrelated to food-borne illnesses can also be detected and enumerated using the appropriate antibodies.

Overall, the combination of device components for scanning a sample during optical analysis provides a good number of tangible benefits of the present instrument. First, use of a confocal microscope in combination with a simple mechanical setup for moving the sample container provides a means for transporting particles through an observation region while avoiding the need for generating a fluid flow. As a result, the sample undergoing analysis does not require extensive prefiltration to prevent problems associated with sample flow and clogging, as in optical flow cytometry systems. In addition, the sample never enters the inner workings of the device, thereby making the present analysis systems less susceptible to problems associated with contamination, bacterial growth, and formation of bio-films. Furthermore, the sample is not lost or damaged during optical analysis, thereby allowing the sample to be subjected to additional and complementary analyses after detection and characterization by the present methods. Second, use of a confocal microscope enables use of very small observation volumes, as small as picoliters, which are useful for ensuring that particles pass through the observation region one at a time and improving signal to noise ratio. Vertical displacement and rotation of the container, however, allow for large volumes of sample,

such as sample volumes equal to about 1 milliliter, to be characterized using relatively short sample scanning periods, of the order of 1 minute. Third, use of a confocal microscope allows an illumination focus to be selected such that the observation region is positioned relatively close (e.g. about 50 microns to about 500 microns) to the walls of the container holding the sample. This feature allows the components of highly scattering media, for example body fluids, to be effectively analyzed using the present device and methods. Fourth, use of a confocal microscope in combination with a means for moving the sample container provides a means for transporting sample containing particles through an observation region without requiring complex optical systems comprising moveable optical components, such as translating optical sources, photodetectors or dichroic mirrors. This aspect of the instrument is advantageous as it provides a simple, mechanically robust experimental system that does not require repeated optical realignment between scans.

Figure 5.6 represents calibration curves, linear and logarithmic, that were obtained from many measurements done over many months with different dilutions of fluorospheres. The laser intensity was variable. The confocal slit was the same throughout. The results are very consistent. This shows that this technique does not require frequent or complicated calibration of the instrument.

For concentrations usually encountered in biotechnological and clinical applications ($10^3 – 10^7$ or more), a few seconds of scanning time is enough for statistically sound results. That usually means the detection of a number of hits of the order of 100 or even less. If scan times of the order of 1 minute are adequate for concentrations of the order of 10 particles /ml, concentrations 3 to 7 orders of magnitude

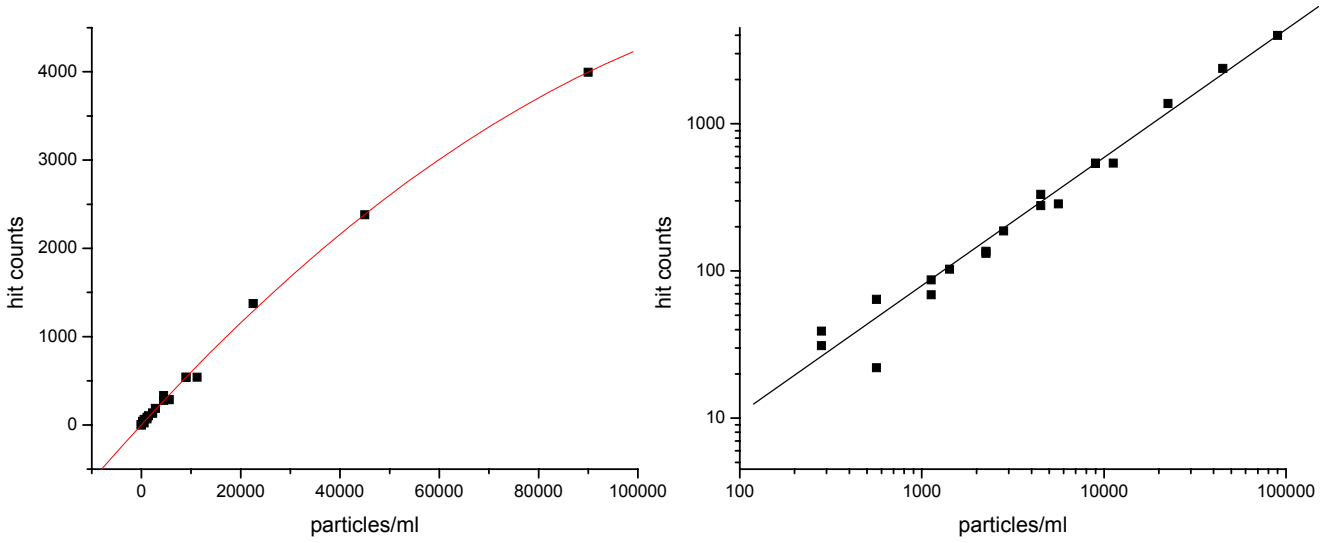

Figure 5.6 The calibration curves, linear and logarithmic, were obtained from many measurements done at different times with different dilutions of fluorospheres. The laser intensity was variable. The confocal slit was the same throughout. This shows that this technique does not require frequent or complicated calibration of the instrument.

higher, as usually encountered in practice, then require scan times the same order of magnitude shorter. The present methods and instrumentation are therefore amenable to computer assisted automation and, thus, are well suited to high throughput optical analysis of a large number of samples.

In the next chapter, I will discuss a very interesting clinical application of our methods. Its ultimate goal is to find a clinical correlation between abundance and size distribution of soluble β-Amyloid oligomers in cerebrospinal fluid of a patient on one hand, and the stage of dementia in Alzheimer's disease on the other. For this purpose, we had to expand our data analysis filtration algorithms to not only detect entities of interest in fluid samples, but in addition to characterize the size distribution of these same entities.

Chapter 6 Further Advances: β-Amyloid Oligomer Detection and Size Characterization

Outline

This chapter describes an ongoing collaboration that required us to further develop and advance the setup and the detection program. I introduce the clinical problem and the goal of finding a diagnostic marker for the progression of Alzheimer's disease. A potential candidate is the size distribution of soluble oligomers of β-Amyloid protein in cerebrospinal fluid and, ultimately, in blood plasma. I describe the modifications introduced in the setup and the new size characterization capabilities of the correlation filter. Some preliminary results are presented.

Background of the Application

The search for Alzheimer's disease biomarkers: Alzheimer's disease (AD) is a neurodegenerative condition that usually starts late in life, although a familial form has an early onset. More than four million people are affected in the United States, resulting in more than 100,000 deaths annually (Terry, Katzman et al. 1999). The Amyloid Hypothesis (Selkoe 1991; Hardy and Higgins 1992; Hardy and Selkoe 2002) has driven the search for new therapeutic approaches and guided the evaluation of biomarkers for the disease. A clear separation between controls and AD patients has not been obtained from total amounts of the β-amyloid peptide in plaques and the tau protein in neurofibrillary tangles (Andreasen and Blennow 2002; Csernansky, Miller et al. 2002;

Frank, Galasko et al. 2003). They are particularly insensitive in early (pre-dementia) disease where the need is greatest for a diagnostic marker.

A correlation between *soluble* Aβ content and synaptic loss is supported by many studies. Increases in soluble Aβ levels have been associated with the severity of neurodegenaration, and distinguish AD from normal and other forms of pathological aging (Lue, Kuo et al. 1999; McLean, Cherny et al. 1999; Wang, Dickson et al. 1999). Indeed evidence of neuronal toxicity due to a histologically invisible form of the β-peptide has been mounting. Under conditions where fibril formation is not detected, the soluble oligomers are significantly more toxic than other forms of the peptide to primary neuronal cultures, brain slice preparations, and when injected intracerebrally (Podlisny, Walsh et al. 1998; Hartley, Walsh et al. 1999; Walsh, Hartley et al. 1999; Kim, Chae et al. 2003).

The toxic activity of soluble Aβ appears to be concentrated in multimeric forms of the peptide (Hartley, Walsh et al. 1999; Dahlgren, Manelli et al. 2002). High molecular weight (oligomeric) soluble Aβ was shown to be greatly increased in AD brain using molecular sieving and centrifugation (Kuo, Emmerling et al. 1996). Measurements with two different oligomer-specific antibodies suggest increased levels of oligomer immunoreactivity in AD brain lysates (Gong, Chang et al. 2003; Kayed, Head et al. 2003) compared to controls.

Assay of characteristic soluble oligomeric pathologic proteins has been proposed as a diagnostic for chronic neurodegenerative diseases (El-Agnaf, Walsh et al. 2003). Despite their propensity to elicit biological effects at physiologic concentrations, oligomeric forms of Aβ represent only a small fraction of the total soluble Aβ peptide

(Gong, Chang et al. 2003; Kayed, Head et al. 2003). Although methods such as Sandwich ELISA can be used to detect oligomeric Aβ (Howlett, Cutler et al. 1997; El-Agnaf, Mahil et al. 2000), the size distribution of oligomers, which may turn out to be an important parameter, cannot be distinguished. An ideal technique would be one which combines high sensitivity with the capability of distinguishing size classes of oligomers.

Fluorescence Correlation Spectroscopy (FCS) has been used to detect oligomeric complexes of the Aβ peptide in vitro aggregation studies (Tjernberg, Pramanik et al. 1999; Sengupta, Garai et al. 2003), and in CSF of AD patients (Pitschke, Prior et al. 1998; Bark, Tjernberg et al. 2002). By utilizing the selective association of fluorescently-labeled Aβ peptides with preformed aggregates of Aβ peptide and the single molecule detection capability of the technique, low abundance large Aβ oligomers were identified by their brightness and small apparent diffusion coefficient (size) and by their removal by immunoadsorption of the CSF with an Aβ-specific antibody. The same technique has been applied to another self-oligomerizing system, prion proteins (Post, Pitschke et al. 1998), and a two-color correlation method with differently labeled antibodies can detect sub-infectious dose levels of prion oligomers (Bieschke, Giese et al. 2000).

Although FCS based on diffusion established the concept that CSF oligomers could be diagnostic for AD, improvements in instrument robustness, software analysis, measurement speed, and extensive clinical studies for correlation with disease severity and other parameters are required. Also, higher sensitivity is required to assay the oligomer content of more accessible biological fluids such as plasma/serum, and urine, and the correlation with disease in these fluids remains to be established. Current

techniques do not sample enough volume to accumulate statistically meaningful particle counts in reasonable time frames.

Significance of our setup: The instrument and analysis method we have designed represent a significant advance in the practical application of FCS technology to the analysis of clinical samples. A system to rapidly, reproducibly, and quantitatively monitor a biomarker for a toxic form of Aβ peptide in a small volume of biologic fluid will 1) allow the assessment of the utility of the marker as an early pre-clinical stage diagnostic tool, 2) reduce the cost and speed the clinical trials of new disease modifying therapeutics, and 3) significantly impact research into the pathogenic mechanism of AD. If levels are correlated with disease progression and oligomers can be monitored in serum/plasma or urine, this information will be useful for diagnostic purposes as well as monitoring the effects of therapeutic agents during clinical trials. The small amount of sample required and the high sensitivity of our setup will allow physiological levels of oligomers to be quantified in mouse models of AD where sample volumes are limited.

There are other potential applications for the determination of oligomeric protein forms in biological fluids beyond Alzheimer's disease. Soluble, toxic, oligomeric forms of misfolded, aberrantly polymerized proteins are a hallmark of a number of neurodegenerative and other diseases (Walker and LeVine 2000). Those impacting the nervous system include Alzheimer's disease, α-synucleinopathies, (e.g. Parkinson's disease, Lewy Body Dementia), tauopathies (e.g. Pick's disease), polyglutamine diseases (e.g. Huntington's disease), amyotrophic lateral sclerosis, the prion diseases (i.e. variant Creutsfeld-Jacob Disease, "mad cow" disease), and cerebrovascular β-amyloid angiopathy. Measurements of specific oligomers with antibodies or selective binding of

the cognate molecule might be useful in diagnosing, monitoring therapy, and in studying the disease process in humans and in animal models.

Filtration Software and Size Characterization

The filtration algorithms were described in chapter 4 as a means of detection of particles and a way of effectively raising the signal-to-noise ratio. These algorithms have been expanded to determine the distribution in size of the particles detected. Traditionally, especially in flow cytometry and related techniques, the forward light scattering is used for the purpose of estimating the diameter of the cells flowing through the excitation volume. For size measurements in the submicron range, where Rayleigh scattering predominates, orthogonal scattering signals are usually used. Both have limitations due to many factors affecting the amount of scattering other than cell size. These include the range of angles over which light is collected, differences in the refractive index between the cells and the suspending medium, the presence of strongly absorbing materials in the cells, and strong dependence on the wavelength of the light used (Shapiro 1995; Davy and Kell 1996). In our setup, it is the time of flight of the extended particle in a smaller observation volume that is used to determine the physical extent of the each particle detected.

Operation of the pattern recognition algorithms is able to classify the particles in the sample on the basis of the physical property of size in addition to the optical property of brightness mentioned earlier. Characteristics of the ensemble of particles, such as the particle size distribution and the particle brightness distribution, are determined by analysis of the amplitudes and shapes of intensity distributions of the predetermined

patterns matched to features in the temporal profile. The width of the predetermined patterns matched to features in the temporal profile, for example the full width at half maximum, can be positively correlated to the residence time of particles in the observation volume. As a result, the size of particles passing through the observation volume may be determined by varying the width of a preselected pattern to quantitatively match features in the temporal profile.

In this context, use of the pattern recognition algorithms provides size analysis methods capable of classifying particles on the basis of size over a wide dynamic range of sizes, such as a range from about 50 nanometers to tens of microns. The program can scan over different widths of the pattern. This feature is used when the size of the particles of interest is not uniform. The program gives the distribution of particle sizes in the sample.

In principle, given the size of the slit, the optical magnification and the rotational velocity, the size can be obtained without a priori calibration. However, calibration with particles of known size can also be used in the present setup.

Preliminary Results

This is collaboration with Dr. Harry LeVine III, Professor at the Department of Molecular and Cellular Biochemistry, Chandler School of Medicine and the Center on Aging, University of Kentucky. The goal is to measure low concentrations of Aβ oligomers in carefully characterized clinical cases participating in a donor program at the Alzheimer's Disease Research Center (ADRC) as part of the Sanders-Brown Center on Aging.

CSF from Alzheimer's disease and age-matched control subjects obtained at autopsy (n=19 AD; n=21 C average postmortem interval <3.5 hrs) were labeled with fluorescein- human Aβ(1-42) (FL42) (Anaspec, Inc.) and assayed by FCS according to methods modified from Pitschke (Pitschke, Prior et al. 1998). Two photon excitation (780 nm, Ti:Sapphire laser, mode-locked, 150 fs pulses, 6 - 9 mW at the sample) was employed to reduce photodamage to the probe and better define the sampling volume. Detection was done with an EG&G model SPCM-AQR-15 avalanche photodiode operated in the photon-counting mode. The laser illumination was focused on a 10 μl sample droplet in an 8-chamber slide (LabTech, cat. 15541) through a 40X NA=1.4 oil objective. Single molecule detection and correlation analysis of fluorescein and fluorescein - lysozyme were used to calibrate the instruments. 16-bit data sampling rates ranged from 16 - 32 kHz to discern single molecule events.

FL-42 in 10 mM NaPi - 0.2% w/v SDS, pH 7.5 was diluted to 100 nM and 0.02% SDS in the CSF sample to label the endogenous oligomeric complexes. Large bright particles were observed in the AD samples above the free fluorescent peptide background. Neither the unlabeled CSF samples nor 100 nM FL-42 in 10 mM NaPi, pH 7.5 generated the large bright oligomers observed in the labeled CSF samples over the time of the measurements.

Static diffusion: The large bright oligomers were detected as rare events, estimated number concentration < 1 pM, consistent with the results of Pitschke et al. (Pitschke, Prior et al. 1998). These large oligomers diffused slowly and most of the sampling time was waiting between events. We would anticipate that the combination of

low concentration and slow diffusion of oligomers would require days for a single determination with sufficient statistics.

Beam scanning & 3-D raster scanning: In order to collect enough events to make meaningful comparisons in minimal time, several beam-scanning paradigms were tested to increase the volume sampled while retaining the resolution to distinguish individual molecules. Without scanning, the confocal image continuously monitored a volume of ~ 1 fl. Scanning the focal point in a 20 μm diameter circle with a 4 msec period sampled a volume of ~ 0.5 pl. Raster scanning 45 x 45 μm in X-Y and 60 μm Z-axis in 3 μm increments sampled ~ 120 pl.

Typical scans for control and AD samples are shown in figure 6.1.

The intense spikes in the top two graphs were interpreted as large oligomeric Aβ complexes based on their slow diffusion (peak width). In this small sample of autopsy CSF samples, the control group (n=22, average 3.105 ± 0.648 peaks S.D.) can be distinguished from the AD group of subjects (n=18, average 6.053 ± 0.800 peaks S.D.) at p=0.00346. Although the groups are separable, the populations overlap, due in part to the small number of events observed. The 3-D scans were converted into a quasi 3-D image, bottom picture, showing a number of large fluorescent oligomers (elongated white spots).

Large volume sample scanning: For this application, the setup of the instrument has been modified in a way to provide the best signal-to-noise ration possible for the detection of soluble β-Amyloid protein aggregates in cerebrospinal fluid. The rotational motion of the cuvette holding the sample is now provided by a 24V synchronous motor

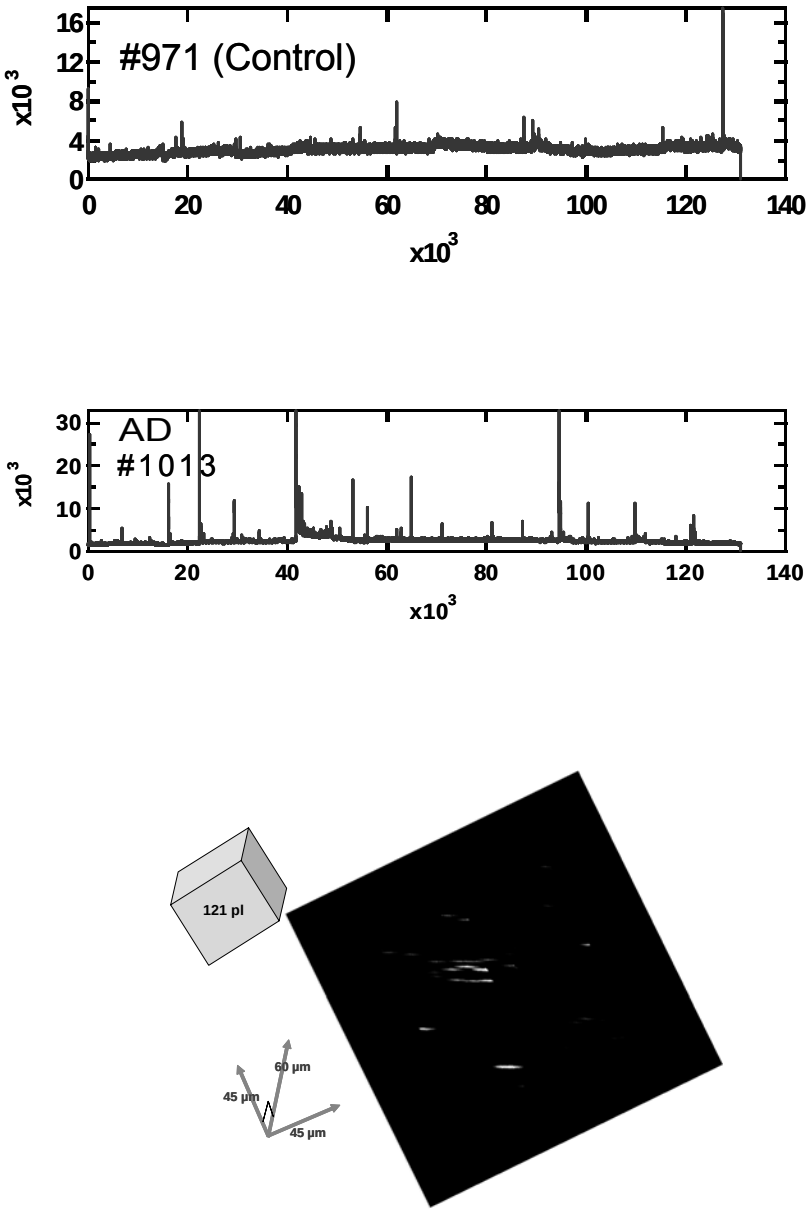

Figure 6.1 2-Photon FCS of FL42 in CSF of control (top) and AD (middle) subjects. The spikes are due to large β-Amyloid complexes. A larger number of spikes is seen in the AD sample.
Bottom: 3D raster scanning converted to an image showing a number of fluorescent Aβ oligomers.

(Hurst Mfg., SA4001-003), fed with a sinusoidal signal from a Synthesized Function Generator (Stanford Research systems, Model DS345), amplified with a Krohn-Hite Amplifier (Model 7500). This provides for a variable rotational speed that can be adjusted at will by varying the frequency of the power signal. This affects the time of flight of the particles in the excitation region, as a slower rotational speed of the cuvette means the particle spends a longer time being observed. A smaller slit (Melles Griot, 25 μm) was used to restrict more the observational volume. This was done for two reasons. One is for a better signal to noise ratio for better detection of the oligomers. The second is for better sizing of these aggregates as the width of the image of the slit needs to be smaller than the extent of the oligomers. Of course, this reduces the total volume scanned in one measurement. However, the estimated concentration the β-Amyloid protein aggregates in CSF is in the femtomolar scale (Georganopoulou, Chang et al. 2005). We are sacrificing about 2 orders of magnitude in the volume of PSF, and 1 order in speed of scanning. With one-minute scanning time, and starting from the subattomolar range, that leaves us at the right scale.

Figure 6.2 shows the preliminary results obtained through detection and sizing with the correlation filter algorithms. The samples were prepared the same way as above. We employed a scanning time of 3 min. The data was analyzed with the correlatin filter program. A basic Gaussian pattern was used. We set the standard deviation value (SDV, width of Gaussian) between 1 (narrow) and 60 (wide). The program scans automatically and repeatedly over the data between the two limits of SDV. Figure 16 shows the SDV values on the x-axis, and the total number of hits for each value on the y-axis.

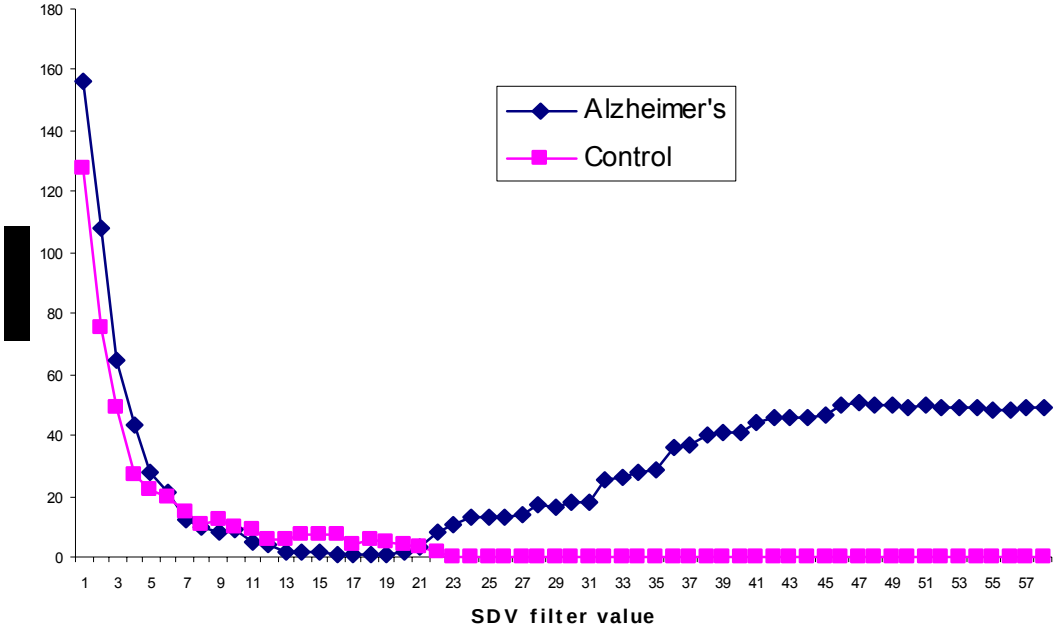

Figure 6.2 Size histograms of β-Amyloid soluble oligomers in the CSF samples from a control and an AD patient. Detection and sizing were done with the correlation filter software

Ignoring noise that comes from small SDV values, the figure clearly shows a different distribution of β-Amyloid oligomer sizes for SDV larger than 25 for control and AD samples.

Chapter 7 Concluding Remarks and Future Prospects

Outline

In this chapter I briefly discuss examples of many potential applications of the device and methods. I also describe some possible and useful expansions such as multichannel setup and multi-slit confocal aperture configuration. Potential setups for continuous monitoring of air and water and the use of bioluminescent bacteria for heavy-metal and toxicity evaluation in environmental and related studies are mentioned.

General Technique with Many Applications

In this dissertation, I have described an alternative technology for the detection and enumeration of extremely low concentrations of fluorescently-tagged particles in both clear and scattering media. The technical methods and the device built aim for large dynamic range in terms of the size of the entities to be studied, low cost, simplicity, and portability. In addition to describing the instrument and the techniques used for detecting particles in a sample and measuring concentrations, I have described the application-driven evolution of the system to the present status where it can also determine the size distribution of the entities measured. I have shown that a combination of the large volume of exploration, the regular motion of the sample, and the pattern recognition algorithms, resulted in unprecedented sensitivity for the detection of a small number of particles in a relatively large volume without the need of enrichment steps.

The high degree of versatility with respect to the composition of materials analyzed by the present instrumentation and techniques, makes these suitable for a wide range of applications including, but not limited to, characterizing cellular material and microorganisms, identifying biological molecules present in biological samples, assaying materials present in food stuff, detection of pathogens in samples, assaying of biological samples for clinical diagnostic and therapeutic applications, high throughput quantitative analysis of samples, and functional assays for monitoring protein expression rates.

Possible uses of the system are in:

1. clinical applications
2. food industrial applications
3. pollution monitors
4. water and air quality control
5. biodefense monitors

Possible Expansions

In addition to improving the instrument by having an adjustable rotational velocity for optimum signal to noise ratio as mentioned in the last chapter, making the vertical motion simpler by the use of an eccentric plate mechanism for more compactness, and improving the particle passage recognition software for better detection and sizing, other ideas for expanding the setup are mentioned here for future consideration.

Multi-channel setup:

This aspect will provide for a setup for selectively detecting and measuring the concentration of particles in a fluid sample capable of discriminating between particles having different physical and/or chemical properties.

The planned expansion provides multichannel optical analyzers capable of simultaneously and independently monitoring fluorescence from a number of different fluorescent probes associated with particles transported through the observation region.

In one embodiment, a plurality of fluorescent probes having different emission wavelengths is provided to the fluid sample undergoing analysis. The composition of each fluorescent probe is chosen such that it associates selectively with materials of interest in the sample, for example by using a plurality of different nucleic acid fluorophores or fluorescent antibodies that selectively bind to different surface or intracellular proteins or peptides. Excitation by light from one or more optical sources causes particles labeled with one or more probes to fluoresce. The intensities and wavelength distribution of the fluorescence depends on the abundances and identities of fluorescent probes associated with the particles, and thus, can be used to classify the particles on the basis of composition, all in a single experimental run. A plurality of photodetectors is provided with wavelength discrimination elements, such as optical emission filters and dichroic reflectors, such that each are capable of detecting the fluorescence originating from a selected fluorescent probe and do not detect fluorescence originating from other fluorescent probes associated with the particle. Accordingly, each photodetector in this optical arrangement independently generates a temporal profile of

fluorescence from the observation volume corresponding to a selected fluorescent probe. See figure 7.1.

This setup is also beneficial for another reason. It provides better detection specificity, as the particles of interest may be tagged with more than one fluorescent probe emitting in different regions of the electromagnetic spectrum. Analysis of the output of two or more photodetectors for coincident detection events allows for discriminate detection and quantification of the particles of interest.

Multi-channel setup for size distribution:

In this regard, the idea is to have multichannel optical analyzers where a number of photodetectors is provided each having a differently sized confocal aperture in optical communication with the confocal microscope. In this setup, the photodetectors detect light from observation volumes having different effective focal volumes. Analysis of fluorescence temporal profiles from observation volumes corresponding to different effective focal volumes aids in better resolving the size distribution of particles in the sample because the size of the particle will change the transit time through the confocal slit. Different confocal apertures can be used to determine the size of the particle more accurately.

Use for continuous monitoring of air and water:

The idea here is to make possible measurements of the concentrations of particles introduced to a fluid sample undergoing optical analysis. In this aspect, the container holding the sample is connected to a means of introducing particles into the sample. For

example, a tube is provided to the container for bubbling gas through the sample or introducing fluids prior to or during optical analysis. Alternatively, a fluid introduction system may be connected to the container capable of providing drops of liquid containing particles to the sample. In these realizations, particles are systematically provided to the container, continuously or at regular intervals. The optical analysis device of the present setup periodically probes the sample, thereby providing measurements of the concentrations of particles that accumulate in the fluid sample. This aspect of the instrument is particularly useful for detecting pathogens in environmental samples, such as room air, as in surgical operations rooms in hospitals, or water samples from city water supplies.

Use of bioluminescent bacteria for heavy-metal detection and toxicity evaluation:

Our device and methods are also broadly applicable to optical analysis of particles undergoing emission other than fluorescence, such as via photoluminescence, chemiluminescence and or electroluminescence processes. For example, the present device and methods are useful for identifying, classifying and determining the concentration of particles capable of undergoing chemiluminescence or bioluminescence. Emission from particles passing through the observation volume of the confocal microscope is collected, detected and analyzed without the need for providing excitation light to the sample.

A very useful biotechnological example is the use of bioluminescent bacteria for the purpose of heavy metal detection and toxicity determination in environmental and other studies. Bioluminescence refers to the light emission from living organisms that

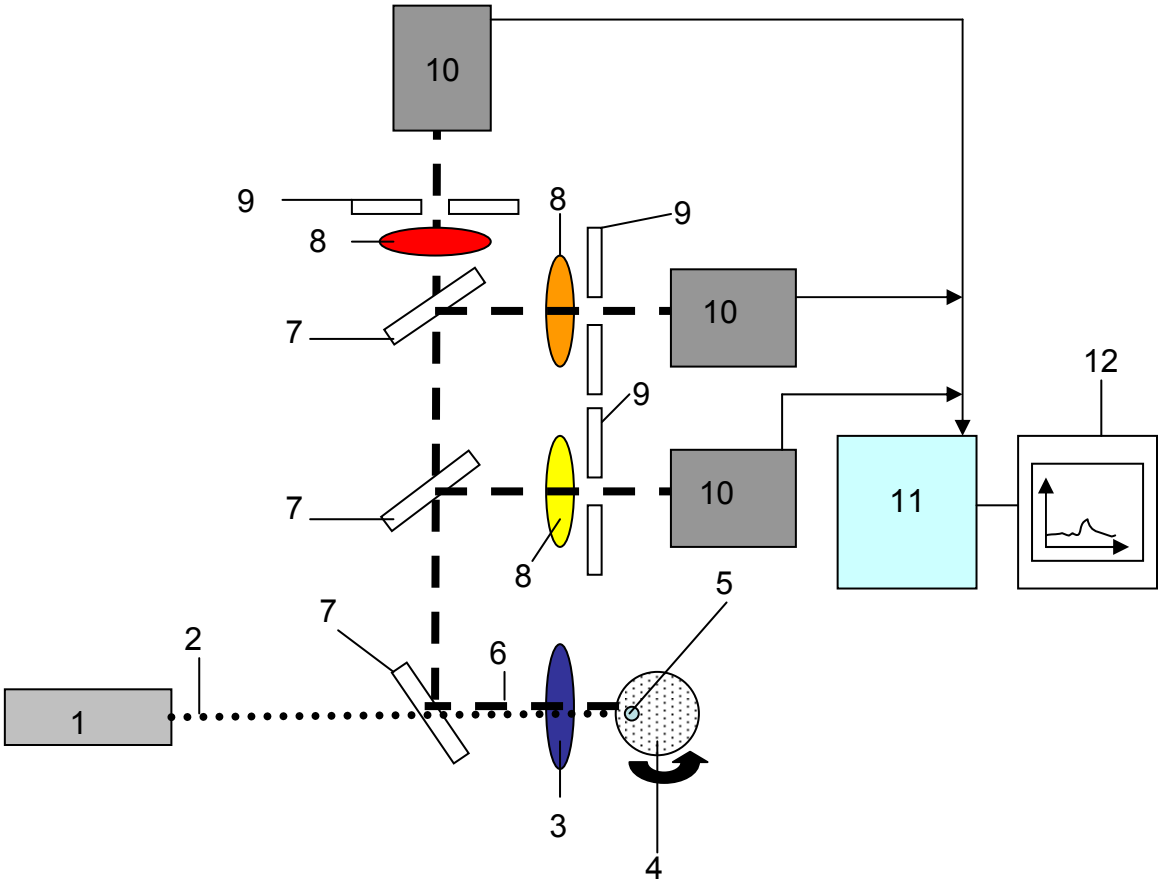

Figure 7.1 Sketch of proposed Multichannel setup
1 laser source, 2 excitation light, 3 microscope objective, 4 cuvette holding sample, 5 excitation focus, 6 fluorescence emission, 7 dichroic mirrors, 8 emission filters, 9 confocal apertures, 10 photodetectors, 11 computing processor, 12 display

accompanies the oxidation of organic compounds mediated by the enzyme catalyst luciferase. The expression of luminescence in many bacteria is highly dependent on cell number density. It is observed only when bacteria are at high concentrations such as in the light organs of certain fish and squid (Bulich 1986; El-Alawi, McConkey et al. 2002; Perego, Fanara et al. 2002).

The bacteria luminescence reaction in the form of light at 490 nm, involves the oxidation of aliphatic aldehyde and reduced flavin mononucleotide:

$$FMNH_2 + RCHO + O_2 \rightarrow FMN + RCOOH + H_2O + light$$

Toxic substances in small quantities can inhibit this biochemical process of light emission; therefore their effect can be detected with high sensitivity by means of residual luminescence.

A specific strain of marine aerobic Gram negative bacteria, *Vibrio fischeri*, has been successfully employed as a high sensitive indicator of the presence of several chemicals at various concentrations: heavy metals, phenols, narcotics, waste toxins, pesticides, medicines…(Bulich 1986; El-Alawi, McConkey et al. 2002; Perego, Fanara et al. 2002) The method is based on the quenching of bioluminescence of the bacteria by the different toxicants. The amount of luminescence from a reactivated sample of bacteria is measured. The bacteria are then transferred to a toxic sample solution and the bioluminescence is measured at different time intervals. The time-dependent decrease in the luminescence is an indicator of the degree of toxicity. Standard protocols and calculations are followed and used for this determination.

Statistically, bioluminescent bacteria give better results than other bioassays because of the large bacteria involved. In addition, bacteria are more economical as they

are easier to culture and preserve. Our setup may provide another advantage as the luminescence from individual bacteria can be measured, and not just an ensemble average. This might lead to a better sensitivity for this kind of tests.

Multi-Slit Confocal Aperture for Better Localization and Intrinsic Brightness Determination

One important particular expansion for our instrument involves producing a method to better determine the position of the particle in the beam without sacrificing the large volume of exploration, which is needed to achieve ultra-high sensitivity. If we could determine the position of the particle, we could remove the uncertainty about the absolute intensity of the particle. When a particle passes through the observation volume, the measured fluorescence depends on the intrinsic brightness of the particle and the specific position of its trajectory in the illumination profile, the intensity being higher closer to the center of the confocal volume.

A different approach is proposed where we use an optical principle to determine the position of the particle with respect to the center of the illumination profile. This approach uses multiple slits in front of the detector instead of the single slit we have now in our device. In relation the figure 7.2, consider what is happening if a particle passes exactly in the center of the confocal volume (A) or away from the center (B). As the particle passes away from the center, the width of the fluorescence burst increases, providing a simplified mapping of the particle position as a function of the width of the recorded burst. The precise determination of the particle position can be increased if we use multiple slits. For the case of two slits, when the particle passes exactly at the center

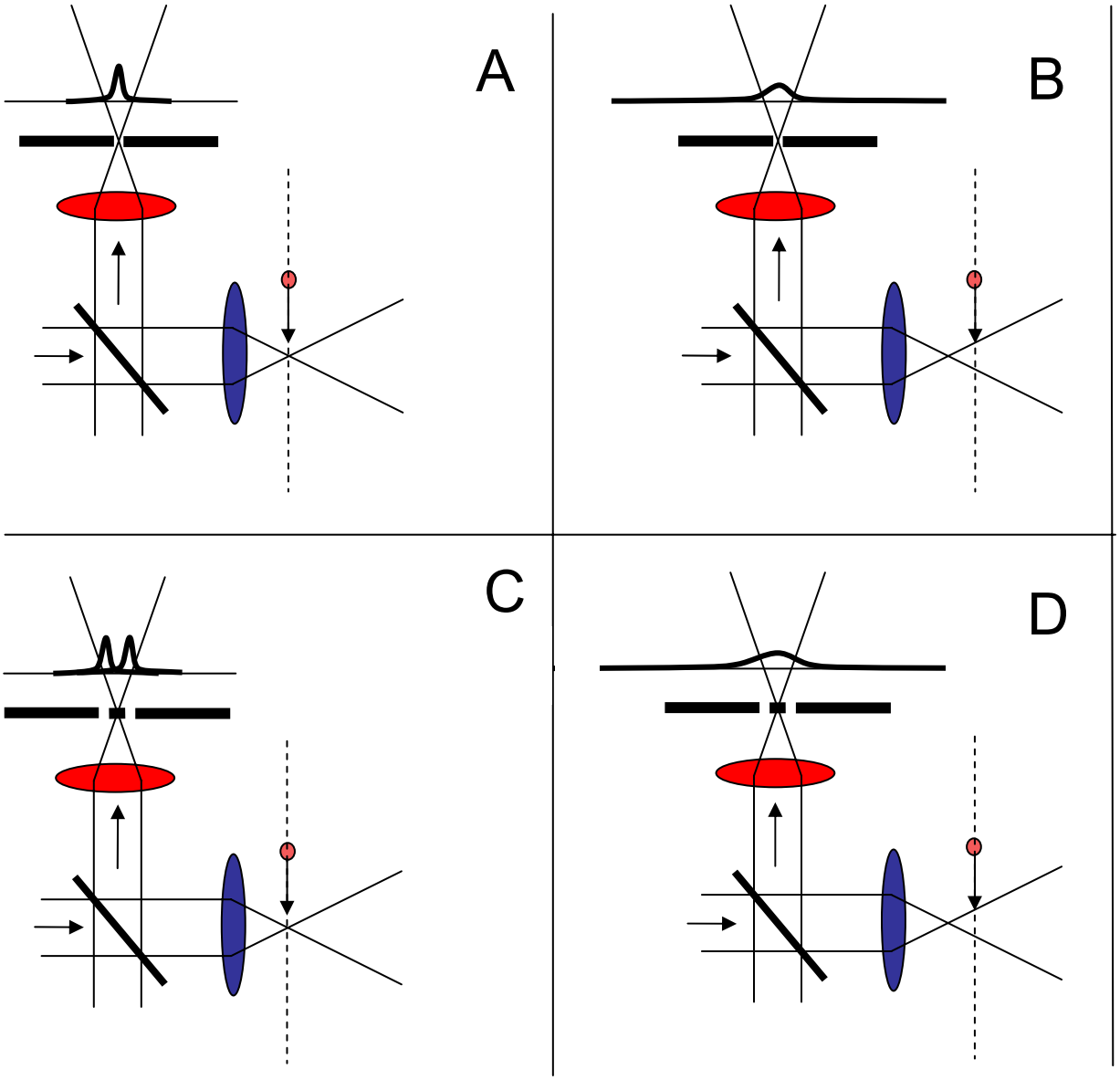

Figure 7.2 Multislit confocal aperture

With one slit, points in focus give one peak; points out of focus give a broad peak.

With two slits, points in focus give two peaks; points out of focus give a broad peak

of the confocal volume we have two identical sharp fluorescence bursts (C). As the particle has a trajectory away form the center, the two peaks broaden and eventually merge in a single broad peak (D).

The pattern recognition filter can recognize the different intensity profiles and properly assign the z-coordinate to each particle. Once the z-coordinate is known, we can more precisely calculate the particle intensity. Note that our goal is not to find out the particle trajectory, but to compensate for the illumination intensity. Using this new approach, there is still indetermination, reflection symmetry with respect to the focal plane, which does not affect the calculation of the illumination intensity.

References

Andreasen, N. and K. Blennow (2002). "Beta-amyloid (Abeta) protein in cerebrospinal fluid as a biomarker for Alzheimer's disease." Peptides **23**: 1205-14.

Atlas, R. M. (1984). Use of microbial diversity measurements to assess environmental stress. Current Perspectives in Microbial Ecology. M. J. Klug and C. A. Reddy. Washington, D.C., American Society for Microbiology**:** 450-455.

Bark, N., L. Tjernberg, et al. (2002). "Fluorescence Burst Analysis of Cerebrospinal Fluid as a Diagnostic Tool for Alzheimer's Disease." 8th International Conference on Alzheimers Disease and Related Disorders: Abstr 1382.

Bieschke, J., A. Giese, et al. (2000). "Ultrasensitive detection of pathological prion protein aggregates by dual-color scanning for intensely fluorescent targets." Proc Natl Acad Sci U S A **97**: 5468-73.

Black, J. G. (1996). Microbiology, Principles and Applications. NJ, Prentice Hall.

Bulich, A. A. (1986). Bioluminescence assays. Toxicity Testing Using Microorganisms. G. Bitton and B. J. Dutka. Boca Raton, FL, CRC Press. **1:** 57-73.

Bulich, A. A. (1986). Reliability of bacterial luminescence assay fro determination of the toxicity of pure compunds and comples effluents. Aquatic Toxicity and Hazard Assessment. D. R. Brandson and K. L. Dickson. Philadelphia, PA**:** 338-347.

Cerrusi, A. (1999). Quantitative Frequency-domain Fluorescence Spectroscopy in Tissues and Tissue-like Media. Physics, University of Illinois, Urbana-Champaign.

Chen, Y. (1999). Analysis and Applications of Fluorescence Fluctuation Spectroscopy. Biophysics and Computational Biology, University of Illinois, Urbana-Champaign.

Chen, Y., J. D. Muller, et al. (1999). "The Photon Counting Histogram in Fluorescence Fluctuation Spectroscopy." Biophys. J. **77**: 553-567.

Coulter, W. H. (1956). "High speed automatic blood cell counter and cell size analyzer." Proc. Natl. Electronics Conf. **12**: 1034.

Csernansky, J. G., J. P. Miller, et al. (2002). "Relationships among cerebrospinal fluid biomarkers in dementia of the Alzheimer type." Alzheimer Dis. Assoc. Disord. **16**: 144-9.

Dahlgren, K. N., A. M. Manelli, et al. (2002). "Oligomeric and fibrillar species of amyloid-beta peptides differentially affect neuronal viability." J. Biol. Chem. **277**: 32046-53.

Davy, H. M. and D. B. Kell (1996). "Flow Cytometry and Cell Sorting of Heterogenous Microbial Populations: The Importance of Single-cell Analyses." Microbial reviews **60**: 641-696.

Edwards, C. (1999). Environmental Monitoring of Bacteria. Totowa. NJ, Human Press.

Eigen, M. and R. Rigler (1994). "Sorting single molecules: Application to diagnostics and evolutionary biology." Proc Natl Acad Sci U S A **91**: 5740-47.

El-Agnaf, O. M., D. S. Mahil, et al. (2000). "Oligomerization and toxicity of beta-amyloid-42 implicated in Alzheimer's disease." Biochem. Biophys. Res. Commun. **273**: 1003-7.

El-Agnaf, O. M., D. M. Walsh, et al. (2003). "Soluble oligomers for the diagnosis of neurodegenerative diseases." **2**: 461-2.

El-Alawi, Y. S., B. J. McConkey, et al. (2002). "Measurement of Short- and Long- Term Toxicity of Polycuclic Aromatic Hydrocarbons Using Luminescent Bacteria." Ecotoxicology and Enviromental Safety **51**: 12-21.

Elson, E. L. and D. Magde (1974). "Fluorescence Correlation Spectroscopy, I. Conceptual Basis and Theory." Biopolymers **13**: 1-27.

Elson, E. L., D. Magde, et al. (1974). "Fluorescence Correlation Spectroscopy, II. An Experimental Realisation." Biopolymers **13**: 29-61.

Farber, J. M. and P. I. Peterkin (1991). " Listeria monocytogenes, a food-borne pathogen." Microbiol. Rev. **55**: 476-511.

Frank, R. A., D. Galasko, et al. (2003). "Biological markers for therapeutic trials in Alzheimer's disease." Neurobiol Aging **24**: 521-36.

Georganopoulou, D. G., L. Chang, et al. (2005). "Nanoparticle-based detection in cerebral spinal fluid of asoluble pathogenic biomarker for Alzhimer's disease." PNAS **102**(7): 2273-76.

Gong, Y., L. Chang, et al. (2003). "Alzheimer's disease-affected brain: Presence of oligomeric A{beta} ligands (ADDLs) suggests a molecular basis for reversible memory loss." Proc Natl Acad Sci U S A **100**: 10417-10422.

Hardy, J. and D. J. Selkoe (2002). "The Amyloid Hypothesis of Alzheimer's Disease: Progress and Problems on the Road to Therapeutics." Science **297**: 353-356.

Hardy, J. A. and G. A. Higgins (1992). "Alzheimer's Disease - The Amyloid Cascade Hypothesis." Science **256**: 184-185.

Harmon, R. J. (2001). "Somatic Cell Counts: a Primer." National Mastitis Council Annual Meeting Proceedings.

Hartley, D. M., D. M. Walsh, et al. (1999). "Protofibrillar intermediates of amyloid beta-protein induce acute electrophysiological changes and progressive neurotoxicity in cortical neurons." J. Neurosci. **19**: 8876-84.

Heritage, J., E. G. V. Evans, et al. (1996). Introductory Microbiology. Cambridge, University Press.

Howlett, D., P. Cutler, et al. (1997). "Hemin and related porphyrins inhibit beta-amyloid aggregation." FEBS Lett. **417**: 249-51.

Jay, J. M. (1992). Modern Food Microbiology. NY, Van Nostrand Reinhold.

Kayed, R., E. Head, et al. (2003). "Common structure of soluble amyloid oligomers implies common mechanism of pathogenesis." Science **300**: 486-9.

Kim, H. J., S. C. Chae, et al. (2003). "Selective neuronal degeneration induced by soluble oligomeric amyloid beta protein." Faseb. J. **17**: 118-20.

Kuo, Y. M., M. R. Emmerling, et al. (1996). "Water-soluble Abeta (N-40, N-42) oligomers in normal and Alzheimer disease brains." J. Biol. Chem. **271**: 4077-81.

Lue, L. F., Y. M. Kuo, et al. (1999). "Soluble amyloid beta peptide concentration as a predictor of synaptic change in Alzheimer's disease." Am. J. Pathol. **155**: 853-62.

McDougald, D., S. A. Rice, et al. (1998). "Nonculturability: adaptation or debilitation." FEMS Microbiol. Ecol. **25**: 1-9.

McFeters, G. A., F. P. Yu, et al. (1995). "Physiological assessment of bacteria using fluorochromes." J. Microbiol. Methods **21**: 1-13.

McLean, C. A., R. A. Cherny, et al. (1999). "Soluble pool of Abeta amyloid as a determinant of severity of neurodegeneration in Alzheimer's disease." Ann. Neurol. **46**: 860-6.

Mead, P. S., L. Slutsker, et al. (1999). "Food-Related Illness and Death in the United States." Emerging Infectious Diseases **5**(5): 607-625.

Meyer, T. and H. Schindler (1988). "Particle counting by fluorescence correlation spectroscopy. Simultaneous measurement of aggregation and diffusion of molecules in solutions and membranes." Biophs. J. **54**: 983-993.

Paul, J. H. (1993). The advances and limitations of methodology. Acquatic Microbiology. T. E. Ford. Oxford, Blackwell Scientific**:** 15-46.

Perego, P., L. Fanara, et al. (2002). "Applications of Luminous Bacteria on Environmental Monitoring." Chem. Biochem. Eng. Q. **16**(2): 87-92.

Pitschke, M., R. Prior, et al. (1998). "Detection of single amyloid beta-protein aggregates in the cerebrospinal fluid of Alzheimer's patients by fluorescence correlation spectroscopy [see comments]." Nat. Med. **4**: 832-4.

Podlisny, M. B., D. M. Walsh, et al. (1998). "Oligomerization of endogenous and synthetic amyloid beta-protein at nanomolar levels in cell culture and stabilization of monomer by Congo red." Biochemistry **37**: 3602-11.

Porter, J., R. Pickup, et al. (1997). "Evaluation of Flow Cytometric Methods for the Detection and Viability Assessment of Bacteria from Soil." Soil Biol. Biochem. **29**: 91-100.

Post, K., M. Pitschke, et al. (1998). "Rapid acquisition of beta-sheet structure in the prion protein prior to multimer formation." Biol. Chem. **379**: 1307-17.

Qing, D.-K., M. P. Menguc, et al. (2003). "Connective- diffusion -based fluorescence correlation spectroscopy for detection of a trace amount o E. coli in water." App. Optics **42**: 2987-2994.

Rigler, R. (1995). "Fluorescence correlations, single molecule detection and large number screening: Applications in biotechnology." J. Biotechnology **41**: 177-186.

Saleh, A. (1978). Photoelectron statistics, with applications to spectroscopy and optical communications. Berlin, Springer-Verlag.

Schwartz, A., G. E. Marti., et al. (1998). "Standardizing Flow Cytometry: A Classification System of Fluorescence Standards Used for Flow Cytometry." Cytometry **33**: 106-114.

Selkoe, D. J. (1991). "The Molecular Pathology of Alzheimer's Disease." Neuron **6**: 487-498.

Sengupta, P., K. Garai, et al. (2003). "The Amyloid beta Peptide (Abeta(1)(-)(40)) Is Thermodynamically Soluble at Physiological Concentrations." Biochemistry **42**: 10506-10513.

Shapiro, H. M. (1995). Practical flow cytometry. N.Y., Wiley-Liss.

Shapiro, H. M. (2000). "Microbial analysis at the single-cell level: tasks and techniques." J. Microbiol. Methods **42**: 3-16.

Terry, R. D., R. Katzman, et al., Eds. (1999). Alzheimer disease. Philadelphia, Lippincott Williams and Wilkins.

Thompson, N. L. (1991). Fluorescence Correlation Spectroscopy. Topics in Fluorescence Correlation Spectroscopy. J. R. Lakowicz. NY, Plenum. **1**.

Thorns, C. J. (2000). "Bacterial food-borne zoonoses." Rev. Sci. Technol. **19**: 226-239.

Tjernberg, L. O., A. Pramanik, et al. (1999). "Amyloid beta-peptide polymerization studied using fluorescence correlation spectroscopy." Chem. Biol. **6**: 53-62.

Tortora, G. J., B. R. Funke, et al. (1998). Microbiology, An Introduction. Menlo Park, CA, Addison Wesley Longman, Inc.

Tsien, R. Y. and A. Waggoner (1995). fluorophores for Confocal Microscopy, Photophysics and Photochemistry. Handbook of Biological Confocal Microscopy. J. B. Pawley. NY, Plenum Press**:** 267-279.

Tunlid, A. and D. C. White (1992). Biochemical analysis of biomass, community structure, nutritional status and metabolic activity of microbial communities in soil. Soil Biochem. G. Stotsky and J. M. Bollag. NY, Marcel Decker. **7:** 229-262.

Walker, L. C. and H. LeVine (2000). "The cerebral proteopathies: neurodegenerative disorders of protein conformation and assembly." Mol. Neurobiol. **21**: 83-95.

Walker, S. (1999). In vitro and in vivo image and optical property reconstruction from noninvasive measurements of turbid media: a promising method for optical mammography. Urbana, University of Illinois.

Walsh, D. M., D. M. Hartley, et al. (1999). "Amyloid β-Protein Fibrillogenesis. Structure and biological activity of protofibrillar intermediates." J. Biol. Chem. **274**: 25949-25952.

Wang, J., D. W. Dickson, et al. (1999). "The levels of soluble versus insoluble brain Abeta distinguish Alzheimer's disease from normal and pathologic aging." Exp. Neurol. **158**: 328-37.

Ward, D. M., M. M. Bateson, et al. (1992). Ribosomal RNA analysis of microorganisms as they occur in nature. Advances in microbial ecology. K. C. Marshall. N.Y., Plenum Press. **12:** 219-286.

Winogradsky, S. (1949). Microbiologie du Sol, Problemes et Methodes, Barneoud Freres, France.

Author's Biography

Abdel K. Tahari was born in Bou-saada, Algeria. After high school, he studied for two years in the Department of Engineering at the University of Setif, Algeria. He then moved to Algiers and earned a B.S. in Theoretical Physics at the University of Sciences and Technology, Algiers. Awarded a governmental scholarship, he came to the U.S. and earned an M.S. in Physics at the University of California, Riverside. After teaching Math and Physics at the college level for a few years in California, he joined the Physics Department and subsequently the Medical Scholars Program at the University of Illinois, Urbana-Champaign.